

AEDC-TR-61-8

C-1

Y
J

DEC 20 1961

OCT 1 1961

OCT 8 1969

OCT 14 1971

Approved for public release; distribution unlimited.

**VERIFICATION OF A THEORETICAL METHOD
OF DETERMINING DISCHARGE COEFFICIENTS
FOR VENTURIS OPERATING
AT CRITICAL FLOW CONDITIONS**

By

Robert E. Smith, Jr. and Roy J. Matz
RTF, ARO, Inc.

September 1961

Approved for public release; distribution unlimited.

PROPERTY OF U. S. AIR FORCE
AEDC 61-8
AF 40(6.2)320

**ARNOLD ENGINEERING
DEVELOPMENT CENTER**

AIR FORCE SYSTEMS COMMAND



Additional copies of this report may be obtained from

ASTIA (TISVV)
ARLINGTON HALL STATION
ARLINGTON 12, VIRGINIA

note

Department of Defense contractors must be established for ASTIA services, or have their need-to-know certified by the cognizant military agency of their project or contract.

VERIFICATION OF A THEORETICAL METHOD
OF DETERMINING DISCHARGE COEFFICIENTS
FOR VENTURIS OPERATING
AT CRITICAL FLOW CONDITIONS

By

Robert E. Smith, Jr. and Roy J. Matz
RTF, ARO, Inc.

Approved for public release; distribution unlimited.

September 1961

ARO Project No. 931002

Contract No. AF 40(600)-800 S/A 24(61-73)

ABSTRACT

When the accurate measurement of the flow rates of air or gases is required, the use of a venturi flowmeter which operates at critical flow conditions has certain advantages. A venturi contour designed specifically for use at critical flow conditions is described, and a theoretical method is presented for determining the discharge coefficient of this venturi.

An experimental investigation was conducted to determine the discharge coefficient of such a venturi, and the results are compared with the theoretical values. This investigation covered a range of Reynolds number from 0.4×10^6 to 5.4×10^6 based on venturi throat diameter. The venturi used had a throat diameter of 5.6436 in. and, therefore, an airflow capacity of 8.6 lb/sec at an inlet total pressure of one atmosphere and an inlet total temperature of 519°R. The values of discharge coefficient ranged from 0.992 to 0.994, and the theoretically and experimentally determined coefficients agreed within ± 0.06 percent over the range of conditions investigated.

CONTENTS

	<u>Page</u>
ABSTRACT	3
NOMENCLATURE	7
INTRODUCTION	9
ADVANTAGES OF MEASURING FLOW RATES AT CRITICAL FLOW CONDITIONS	10
DESIGN OF VENTURI CONTOUR FOR OPERATION AT CRITICAL FLOW CONDITIONS	12
THEORETICAL DETERMINATION OF VENTURI DISCHARGE COEFFICIENT	16
EXPERIMENTAL DETERMINATION OF VENTURI DISCHARGE COEFFICIENT	20
COMPARISON OF THEORETICAL AND EXPERIMENTAL VALUES OF VENTURI DISCHARGE COEFFICIENT	25
LIMITATIONS OF METHOD	25
CONCLUSIONS	26
REFERENCES	27

ILLUSTRATIONS

Figure

1. Ideal Mach Number Distribution along Venturi Length at Typical Subcritical and Critical Flow Conditions . . .	29
2. Ideal Weight Flow per Unit Area at Venturi Throat as a Function of Throat Pressure Ratio and Mach Number: Air, $\gamma = 1.40$	30
3. Variation of Ideal Venturi Throat Static Pressure with Maximum Mach Number in Venturi: $\gamma = 1.40$	31
4. Schematic of Venturi Design for Operation at Critical Flow Conditions.	32
5. Details of Venturi Used for Investigation.	33
6. Theoretical Values of Venturi Throat Turbulent Boundary Layer and Displacement Layer Thickness. . .	35
7. Theoretical Mach Number Distribution along Venturi Wall for One-Dimensional and Axisymmetric Flow . . .	36
8. Effect of Theoretical Values of Displacement Layer Thickness on Effective Flow Area at Venturi Throat . .	37

<u>Figure</u>		<u>Page</u>
9.	Theoretical Variation of Mach Number, Static Pressure, and Weight-Velocity across Venturi Throat	38
10.	Schematic Representation of Flow Defects at Venturi Throat	39
11.	Theoretical Values of Venturi Discharge Coefficient. . .	40
12.	Venturi Installation	41
13.	View of Downstream End of Honeycomb Assembly. . . .	42
14.	Flow Straightening Screen Assembly (Looking Upstream)	43
15.	Instrumentation Locations (Looking Upstream)	44
16.	Traversing Static Pressure Probe at Venturi Throat . .	45
17.	Boundary Layer Rake	46
18.	Total Pressure Profiles at Venturi Inlet	48
19.	Variation of Venturi Throat Conditions as a Function of Overall Venturi Pressure Ratio.	49
20.	Venturi Throat Boundary Layer Total Pressure Profiles	50
21.	Comparison of Theoretical and Experimental Boundary Layer Weight-Velocity Profiles	52
22.	Comparison of Theoretical and Experimental Venturi Effective Throat Area Reduction Resulting from Boundary Layer Effects	53
23.	Comparison of Theoretical and Experimental Mach Number and Weight-Velocity Profiles across Venturi Throat	54
24.	Comparison of Theoretical and Experimental Venturi Discharge Coefficients	56

NOMENCLATURE

A	Area
C_d	Discharge coefficient
d	Venturi throat diameter
$f(P_1, P_{2w})$	Value for the steady, one-dimensional isentropic flow of a perfect gas at the given total and static pressure
g	Gravitational constant
M	Mach number
P	Total pressure
p	Static pressure
R	Gas constant for air
Re	Reynolds number based on ideal stream conditions at venturi throat at critical conditions and diameter of venturi throat
r	Venturi radius (measured normal to centerline)
T	Total temperature
V	Velocity
W	Weight flow rate
x	Distance along venturi centerline measured from plane of throat
y	Distance from venturi wall
γ	Ratio of specific heat at constant pressure to specific heat at constant volume
δ	Boundary layer thickness, distance from wall to point in boundary layer where velocity is approximately equal to local stream velocity
δ^*	Boundary layer displacement thickness $= \frac{1}{(\rho_2 V_2)_{y=\delta}} \int_0^{\delta} [(\rho_2 V_2)_{y=\delta} - \rho_2 V_{2\ell}] dy$
θ	Boundary layer momentum thickness $= \frac{1}{(\rho_2 V_2^2)_{y=\delta}} \int_0^{\delta} \rho_2 V_{2\ell} (V_{2y=\delta} - V_{2\ell}) dy$

μ	Dynamic viscosity
ρ	Density

SUBSCRIPTS

eff	Effective
inlet	Venturi inlet
exit	Venturi exit
l	Local
t	Venturi throat
theo	Theoretical
w	Venturi wall
1,2,3	Station designations

SUPERSCRIPT

*	Conditions at critical velocity for steady, one-dimensional isentropic flow of a perfect gas
---	--

INTRODUCTION

The establishment of techniques to permit the accurate measurement of the quantity of fluid flowing past a fixed point in a given system has been a problem for many years. Many different principles and techniques have been employed in an attempt to perfect an accurate, simple, and reliable technique for making flow measurements in a closed conduit. Today, accurate measurement of flow rates plays a very important role in the development of aircraft and missile propulsion systems for which complete knowledge of the flow rates of the working fluids must be established. Similarly, in many industrial applications, the consumption rates of liquids and gases must be accurately determined. At the present time the venturi (axisymmetric converging-diverging nozzle) is one of the devices most frequently used to measure the rate of flow of large quantities of fluids.

During the past several decades, an increasing amount of effort has been applied to the establishment of standards for fluid flow measurements. The work done during this period has dealt primarily with the flow of incompressible fluids because: (1) the measurement of the flow rate of incompressible fluids comprised a large part of the needs of industry, and (2) an accurate standard, the weigh tank, existed which could be used to calibrate the measurement devices. Thus, most of the present standards of measurement for compressible fluids are based on data obtained using incompressible fluids, and an appeal is made to similarity to permit their use for compressible flow. For the past several years an increasingly urgent need has existed for the establishment of standards for accurate measurement of rates of flow of gases.

The state-of-the-art as of 1955 for measurement of rates of flow of large quantities of gas was evaluated by Cope (Ref. 1); at that time the best accuracy of measurement attainable was to within about ± 1 percent. The minimum tolerance recommended for the discharge coefficient of venturis and nozzles conforming to the latest ASME standards is ± 0.75 percent (Ref. 2). Since additional tolerances must be added for pressure, temperature, and area measurements, the minimum overall tolerance for rates of flow measurement is certainly equal to or greater than ± 1 percent. It is suggested (Ref. 2) that the tolerance on the discharge coefficient can be reduced by calibration of each venturi. However, neither weigh tank calibration facilities nor other direct calibration devices are available which will provide the large gas flow rates which are of interest

for many of the present day military and industrial applications. [Air-flow rates of 8 lb/sec or more at standard venturi inlet conditions (total pressure 2116 psfa, total temperature 519°R) will be considered to be large rates of flow for the purposes of this report.]

A need exists today in many highly critical areas of development and operation of military and industrial equipment for a method of measurement of flow rates of large quantities of gas to within ± 0.25 percent of the true value. As will be shown, one possible way to attain such accuracy of measurement is to utilize a venturi operating at critical flow conditions and venturi discharge coefficients calculated by application of long accepted aerodynamic principles. Presently accepted standards of flow measurement, e. g. Ref. 2, do not include data on discharge coefficients for venturis operating at critical flow conditions.

For the past several years the standard technique for the accurate measurement of large airflow rates (up to approximately 500 lb/sec at standard conditions) used in the Rocket Test Facility (RTF), Arnold Engineering Development Center (AEDC), Air Force Systems Command (AFSC), has been to use venturis operating at critical flow conditions. The discharge coefficients for these venturis have been calculated from theoretical flow considerations. The wealth of experience gained during these years can be used to establish the validity of this theoretical technique so that standards for measurement of flow rates at critical flow conditions can be established.

It must be clearly understood that the discharge coefficient which can be theoretically determined for a venturi will only describe the deviation of the flow rate of real gas through the venturi from the one-dimensional flow rate of a perfect gas. Such a computed coefficient will not take into account errors made in the basic measurements of the pressure and temperature of the flowing gas, the area of the venturi throat, and the thermodynamic properties of the flowing gas.

In this report the design of a satisfactory wall contour for venturis to be used at critical flow conditions is discussed. The methods used to theoretically predict the discharge coefficient of the venturi are presented, and the results of an experimental investigation conducted to determine the discharge coefficients for a venturi operating at critical flow conditions are shown. The theoretical and experimental results are compared.

ADVANTAGES OF MEASURING FLOW RATES AT CRITICAL FLOW CONDITIONS

The Mach number distribution based on the one-dimensional, steady isentropic flow of a perfect gas through a venturi at typical subcritical

and critical flow conditions is shown schematically in Fig. 1. Operation at critical flow conditions is characterized by a continuous acceleration of the flow from the venturi inlet to some station downstream of the minimum area (throat section) of the venturi. Ideal weight flow rate per unit area at the venturi throat is shown in Fig. 2 as a function of throat Mach number and throat pressure ratio. Variation of venturi throat static pressure as a function of maximum venturi Mach number is indicated in Fig. 3.

The major reason why operation of venturis at critical flow conditions yields the most accurate flow rate measurements can be determined from Figs. 2 and 3. Operation at critical flow conditions, as compared with operation at subcritical conditions, results in a marked reduction of the error in flow rate resulting from errors in measured venturi pressures. The rate of change of airflow with respect to Mach number is large at low Mach numbers of the order of 0.2 to 0.4; the rate of change is zero at a Mach number of 1.0. For example, at a Mach number of 0.3, corresponding to a pressure ratio of 1.06 (Fig. 2), an error in total (upstream) pressure of only ± 0.25 percent results in an error of ± 2.0 percent in airflow rate, and an error of ± 0.25 percent in static (throat) pressure results in an error of ∓ 1.8 percent in airflow rate. At critical flow conditions an error in total pressure of ± 0.25 percent results in an airflow rate error of only ± 0.25 percent, and no additional error contribution results from the static pressure measurement. At critical flow conditions the throat static pressure is constant (Fig. 3) and, what is much more important, need not be measured at all because it can be calculated from consideration of the properties of the flowing gas. For a given accuracy of pressure measurement, then, the error in flow rate at Mach number 0.3 is, for the case where the errors are additive, 15 times as great as the error at the critical flow rate.

It is unrealistic to add the errors in flow rate as shown above for the subcritical case if only errors in the pressure indicating system are to be considered. The throat pressure is normally measured differentially with respect to the upstream pressure so that the major portion of the indicating system error in throat pressure has the same sign as the error in upstream pressure; thus, the errors in flow rate resulting from the errors in the two pressures are subtractive. The throat static orifice is located in a region of relatively high velocity, and, therefore, the indicated pressure is strongly affected by flow curvature and by orifice geometry, contamination, and handling damage. The error in throat static pressure which really must be considered is that resulting from the geometry of the static pressure orifice and from the non-one-dimensional flow effects; in this case, the assumed static pressure error of ± 0.25 percent is not unrealistic. Further, this error in sensing the

static pressure bears no relationship to the error in measuring the upstream pressure so that the errors in flow rate may well be additive, and the error ratio of 15 shown above may well be realistic.

DESIGN OF VENTURI CONTOUR FOR OPERATION AT CRITICAL FLOW CONDITIONS

The major questions which must be answered before a venturi contour which is satisfactory for operation at critical flow conditions can be selected follow:

1. Is a venturi (axisymmetric converging-diverging nozzle) rather than a simple nozzle (converging only) required?
2. What factors affect the discharge coefficient of a venturi?
3. What requirements will the use of theoretical techniques to compute the flow field in the venturi throat impose on the selection of venturi geometry?

The venturi is superior to the simple nozzle. The major advantages, insofar as accuracy of measurement is concerned, are that the flow is guided by the walls to a point well downstream of the throat region and that the feedback of downstream pressure disturbances through the boundary layer to the throat is prevented by the large favorable pressure gradient (static pressure decreasing in the direction of flow) in the initial portion of the diverging section. Other advantages of the venturi over the simple nozzle as a device for measurement of flow rate are (1) the much lower pressure loss across the venturi, which is a significant advantage in pressure limited systems, and (2) the greatly reduced exit velocity from the venturi which makes it possible to re-establish uniform, low velocity flow conditions only a short distance downstream of the venturi. Because of the static pressure rise across the shock wave and in the diverging channel downstream of the shock wave, critical flow rates through a venturi can be established on an ideal basis at very low total pressure ratios across the venturi (e. g., see Ref. 3). As will be shown in this report, actual critical flow rates through a venturi can be established at total pressure ratios across the venturi of only 1.15. On the other hand, critical flow in a simple nozzle cannot be established, even on an ideal basis, until a total pressure ratio across the nozzle of the order of 2 is established, and in actual operation a ratio greater than 2 should be required. The value of pressure ratio of 1.15 required for operation of a venturi at critical flow conditions is not significantly different from the value required for operation of orifices and simple nozzles at subsonic conditions.

The six major factors which cause the flow of a real gas through a venturi to differ from the one-dimensional flow of a perfect gas are:

1. Accumulation of a boundary layer along the venturi walls because of the viscous effects of the real gas
2. Variation of weight flow per unit area (weight-velocity) in the radial direction because of the centrifugal forces which exist in the gas as a result of flow through a contracting section
3. Differences between the thermodynamic properties of the real gas and the perfect gas at the throat of the venturi because of thermodynamic imperfections of the real gas
4. Rotation or swirl of the incoming gas because of effects of upstream piping configurations
5. Distortion of the total pressure profile resulting from the effects of upstream piping configurations
6. Pulsation of flow resulting from disturbances in the gas supply system

The last three factors listed above are not inherent to the process of the flow of gas through a venturi, and, in most cases, the effects of factors 4, 5, and 6 on venturi flow conditions can be made completely insignificant by careful attention to the supply system configuration. (One satisfactory supply system configuration is described in this report in the section concerning the experimental phase of this work.)

It is possible to theoretically account for the differences in venturi flow rate which arise as a consequence of item 3 above for non-reacting gases provided experimental data for the thermodynamic properties of the real gas exist. Such differences arise as a consequence of the variation of the specific heats and the supercompressibility of the gas. In addition, for reacting gases the kinetics of the processes must be taken into account. Treatment of these problems is beyond the scope of this report.

The accumulation of boundary layer along the venturi wall and the existence of weight-velocity gradients in the radial direction (factors 1 and 2 above) are inherent to the venturi flow process. The effect of both of these factors on the critical flow rate can be determined theoretically, and therefore, the discharge coefficient for a venturi can be calculated.

The use of theoretical techniques to compute the flow field in the venturi throat requires a venturi contour which yields a minimum difference

between the real gas critical flow rate and the ideal critical flow rate and at the same time provides the maximum reliability in the calculation of the boundary layer and centrifugal force field effects. The calculated value of discharge coefficient for such an optimum contour has the minimum tolerance possible. Experience in the RTF has shown that the sum of the effects of both the boundary layer buildup and the radial weight-velocity gradients can be approximately 0.5 percent ($1 - C_d = 0.005$) at critical flow conditions. Therefore, if a venturi contour is selected so that these two effects can be calculated to within ± 20 percent of the true value, then the venturi discharge coefficient will be known to within ± 0.1 percent of its true value. To measure gas flow rates to within ± 0.25 percent of the true value, the discharge coefficient of the venturi at critical flow conditions must be known to within about ± 0.1 percent because of the tolerances which must be included for pressure, temperature, and area measurements and for gas property determination.

EXAMINATION OF RECOMMENDED STANDARD VENTURI DESIGNS

An examination of currently recommended standard venturi contours, e. g. Ref. 2, discloses two features which make these contours undesirable for use at critical flow conditions when theoretically determined coefficients are to be utilized. They are, first, the use of a cylindrical throat section and second, the use of a constantly varying wall radius of curvature in the converging section. Both of these features greatly increase the complexity and reduce the reliability of the theoretical calculations.

When a cylindrical throat is used, the rate of buildup of boundary layer because of the influence of an essentially zero pressure gradient (static pressure constant in direction of flow) is high compared with the rate of buildup in the converging section, and, therefore, a large boundary layer growth in the cylindrical section must be added to the growth in the converging section. Any increase in the size of the boundary layer effects directly reduces the accuracy of a theoretically determined coefficient. Also, the radius of curvature at the exit of the converging section is generally finite, and if this section is attached to a cylindrical section, the radius of curvature must discontinuously jump to the infinite value of the cylindrical section. Such a shift in the wall curvature requires rapid diffusion of the flow near the wall. In the best circumstances this diffusion process results in very rapid boundary layer buildup because of the adverse pressure gradient (pressure increasing in direction of flow); in the worst case, separation of flow can occur, and/or standing aerodynamic shock wave systems can appear. If such is the case the venturi throat flow conditions cannot be calculated with any degree of certainty, and further, experimentally determined hydraulic coefficients certainly are not applicable.

Most currently recommended standards for venturi wall contours require a shape in the converging section such that the wall radius of curvature is different at each point along the converging section. It is difficult to compute the radial gradients in the flow at the venturi throat under these conditions, and the reliability of such calculations for the case of a widely varying radius of curvature is apt to be less than for a constant radius of curvature.

DESIGN CRITERIA FOR A VENTURI TO BE OPERATED AT CRITICAL FLOW CONDITIONS

For the flow phenomena in the venturi to be as simple as possible and, therefore, for the calculation of the throat flow conditions to have the maximum reliability, the criteria for the critical flow venturi contour are: (1) no cylindrical throat will be used, and (2) the wall radius of curvature will be constant (that is, a circular arc) throughout the contraction section and to a point well downstream of the venturi throat. In addition, the downstream portion of the diverging section will be conical and will begin at the point of tangency to the circular arc.

To select the proper value of wall radius of curvature, the opposing effects of curvature on the boundary layer buildup and weight-velocity gradients in the flow must be considered. For a given venturi contraction ratio, an increase in wall radius of curvature will increase the boundary layer thickness at the venturi throat because of the increased wall length, but at the same time the lesser flow curvature will reduce the weight-velocity gradients in the flow. Any failure of the various theories to predict the exact physical effects will likely be completely random; thus, the maximum reliability of the calculated venturi discharge coefficient is obtained when the effect of boundary layer on the coefficient is equal to the effect of weight-velocity gradients on the coefficient.

Based on preliminary estimates of the magnitudes of the effects of boundary layer and weight-velocity gradients on the discharge coefficient, the radius of curvature for the converging section of the critical flow venturi was selected as 3.635 venturi throat radii. [As will be shown in this report, this value of radius of curvature did not precisely fulfill the requirement given above that the magnitudes of these two effects on the discharge coefficient should be equal.]

The venturi contraction ratio (ratio of inlet area to throat area) should be as large as practical so that the effects of velocity gradients in the incoming flow on the venturi throat flow conditions will be minimized. A contraction ratio of 5.82 was considered satisfactory because for this contraction ratio, the one-dimensional value of inlet Mach number is only 0.1, and the total pressure loss in even completely separated wakes caused by bluff bodies within the incoming flow is only 0.7 percent.

The value of cone angle selected for the downstream portion of the diverging section is not particularly critical. A value of cone half-angle of about 6 deg was determined by some investigators (Ref. 4) to produce maximum diffusion efficiency. In any case the half angle must be kept small enough so that separation of flow does not occur in the diffuser. The cone expansion ratio should be selected to give the desired venturi exit velocity. In general, it is expected that no real gain can be realized by making the expansion ratio greater than the contraction ratio because of subsonic diffusion losses.

A schematic of a venturi designed according to the criteria presented above is shown in Fig. 4.

No unusual mechanical considerations exist for the critical flow venturi. The usual rigidity requirements must be met so that (1) the venturi throat deflections caused by aerodynamic forces will produce throat area changes several orders of magnitude less than the error in the flow coefficient, (2) ordinary handling of the venturi will not result in throat area changes, and (3) the internal surface can be machined to give the desired contour tolerance and surface finish. In general, the contour tolerance should be specified as an allowable variation in the first and second derivatives of the wall contour rather than as limits on the contour coordinates. The tolerance value should be selected so that the resultant variation in the wall radius of curvature produces an insignificant variation in the values of the weight-velocity gradients at the venturi throat. The surface finish should be selected so that the surface roughness is several orders of magnitude less than the throat boundary layer thickness. The operating range of temperature and pressure establishes the material requirements and protective coating requirements for the venturi.

The details of the venturi designed according to the criteria shown in Fig. 4 and used in this investigation are shown in Fig. 5. The throat diameter of 5.6436 in. was based on a specific need in the RTF for a calibration standard for use with airflow measuring nozzles having throat diameters of from 6 to 10 in.

THEORETICAL DETERMINATION OF VENTURI DISCHARGE COEFFICIENT

The venturi discharge coefficient is the ratio of the actual flow rate of a gas through a venturi to the steady-state, one-dimensional isentropic flow rate of a perfect gas. To obtain the actual gas flow rate, the integral $\int_0^A \rho V dA$ must be evaluated at the throat. To evaluate this integral from

theoretical considerations of the venturi flow, the flow must be divided into two regions: (1) the region within which viscous effects are significant (boundary layer) and (2) the region within which viscous effects are not significant and the flow can be treated as irrotational (core). Such a division of a real flow into these two regions was introduced by Prandtl (Ref. 5) and was restricted to flows at high Reynolds numbers. Because this report deals only with large venturis which handle large flow rates of gas, the Reynolds numbers are sufficiently high for this concept of division to be applicable. In addition, long accepted aerodynamic theories exist which permit the determination of local values of density and velocity throughout the boundary layer and the core.

It must be emphasized that a theoretical approach such as that outlined above will yield the highly accurate values of coefficient desired only if the total of all the non-one-dimensional effects on the flow rate are small (approximately 0.5 percent) because uncertainties of the order of 10 to 20 percent must be expected in the results of the theoretical aerodynamic calculations. This theoretical approach should not be used for venturis having wall contours with extremely long converging sections, short radius of curvature at the throat, or discontinuous first or second derivatives of the wall contour near or upstream of the throat.

Dry air was used as the working fluid throughout the investigation discussed in this report. It was assumed that the air pressure levels were sufficiently low and the air temperature levels were sufficiently high so that air could be treated as a thermodynamically perfect gas. However, it must be emphasized that the methods presented are neither restricted to dry air nor to the thermodynamically perfect gas assumption.

DETERMINATION OF BOUNDARY LAYER CONDITIONS AT THROAT

Conditions in the flow region [region (1) above] within which non-one-dimensional flow exists as a result of viscous effects were determined. The boundary layer thickness and boundary layer displacement thickness at the venturi throat were calculated utilizing the method shown in Ref. 6 for subsonic converging radial flow; the results are shown in Fig. 6. This method of calculation is applicable only to flow conditions for which the transition from laminar to turbulent flow occurs a short distance downstream of the inlet of the venturi so that the entire boundary layer may be treated as turbulent. The venturi throat Reynolds number was used as the independent variable (Fig. 6) because the throat value is a generally accepted parameter although the Reynolds number based on length along the venturi wall is actually a more significant parameter. Also, because of its more common acceptance, the value of the air static temperature

at the throat was used to establish the Reynolds number rather than the more correct value (so far as boundary layer phenomena are concerned) which is between the static air temperature and the venturi wall temperature.

The turbulent boundary layer results (Fig. 6) are strictly valid only over a specific range of Reynolds number. The lower Reynolds number limit is reached when a laminar boundary layer exists along a major portion of the converging wall. The upper limit is established by the surface roughness of the venturi; above this limit boundary layer thickness does not decrease with further increases in Reynolds number.

One very important result shown in Fig. 6 is the small change in boundary layer thickness which occurs with a change in Reynolds number. This small change is a result of the effects of the favorable pressure gradient (static pressure decreasing in direction of flow) on boundary layer growth. For the contraction shape used in this study $\delta_{\text{theo}} = f[(\text{Re})^{-0.09}]$ which compares with $\delta_{\text{theo}} = f[(\text{Re})^{-0.2}]$ for flow with a zero pressure gradient (static pressure constant in direction of flow). Thus for a given change in Reynolds number, the increase in boundary layer thickness for this venturi shape (Fig. 4) is less than one-half the value for flow with a zero pressure gradient (the case of flow along a flat plate or through a cylinder).

In the calculation of boundary layer thickness, the Mach number of the gas in the inviscid layer adjacent to the boundary layer should be utilized. To simplify the boundary layer calculation, the Mach number distribution in the converging portion of the venturi was based on one-dimensional flow relationships. The resulting Mach number distribution along the venturi wall is shown in Fig. 7. For comparison, the Mach number distribution along the venturi wall determined for axisymmetric converging flow by the method of Ref. 7 is also shown. The values of Mach number at the wall are somewhat higher for the axisymmetric flow. To determine if the assumption of a one-dimensional Mach number distribution was valid for use in the boundary layer calculation, the displacement layer thickness was calculated at a throat Reynolds number of 2.7×10^6 for both Mach number distributions (Fig. 7); the displacement layer thickness for the axisymmetric flow distribution was only 5 percent greater than the value for the one-dimensional distribution.

If the values of displacement thickness shown (Fig. 6) are utilized, the ratio of effective to actual flow area of the venturi throat as a function of throat Reynolds number can be determined. The theoretical effective throat area ratio and throat area reduction are shown in Fig. 8.

DETERMINATION OF WEIGHT-VELOCITY VARIATION AT THROAT

In the core flow region [region (2)] within which viscous effects are not significant and the flow can be treated as irrotational, a non-one-dimensional flow exists because of the centrifugal forces created by the turning of the flow in the contraction section. The existence of a pressure gradient in the throat which produces a force equal and opposite to the centrifugal force on each elemental volume of the flowing gas is a necessary requirement for the steady flow process. The static pressure distribution across the throat, and, hence, the Mach number, density, and velocity were calculated by the method shown in Ref. 7 for the venturi wall curvature specified (Fig. 4). Somewhat simplified methods of calculating the throat pressure distribution which will give essentially identical results are presented in Refs. 3 and 8. The calculated static pressure, Mach number, and weight-velocity profiles are shown in Fig. 9. Here again the essentially constant value of the ρV product over a wide range of Mach number near a Mach number of one is shown; the variation in ρV is only about 1/40 of the variation in pressure or Mach number.

The effect of the centrifugal forces on the venturi discharge coefficient can be determined by comparing the integral of the calculated weight-velocity profile over the venturi throat area with the one-dimensional value. The ratio of the integrated flow value to the one-dimensional value is 0.9980 for the particular venturi wall curvature used in this investigation (Fig. 4). [Although the results in Fig. 9 are presented as a function of venturi radius for the sake of clarity, it must be emphasized that all integration is performed using values of radius squared (or area).]

VENTURI DISCHARGE COEFFICIENT

The properties of the flow at each point in the venturi throat are now known for operation of the venturi at critical flow conditions. The venturi discharge coefficient is then simply the product of 0.9980 (centrifugal force effect) and the area ratio (boundary layer effect) (Fig. 8a). The flow defects which must be taken into account by the discharge coefficient are shown schematically in Fig. 10. The calculated discharge coefficient for the venturi (Fig. 5) operating at critical flow conditions over a range of Reynolds numbers is shown in Fig. 11.

It should be noted that all the calculations required to obtain the results shown in Fig. 11 are of a simple and routine nature and can be made in a relatively short period of time using a desk calculator. To calculate the discharge coefficients for venturis designed for use with

gases which cannot be assumed to behave as thermodynamically perfect gases or with gases for which tabulations of boundary layer integrals are not available, the use of electronic computing equipment may be required.

EXPERIMENTAL DETERMINATION OF VENTURI DISCHARGE COEFFICIENT

To verify the accuracy of the venturi discharge coefficient (Fig. 11) determined by the foregoing theoretical means, an experimental program was undertaken in which the total and static pressures in the venturi throat were measured to obtain the boundary layer thickness and weight-velocity variation. The venturi used was designed according to the criteria given in Fig. 4.

APPARATUS

Test Article

Details of the test venturi are shown in Fig. 5, and details of the venturi installation are shown in Fig. 12. The 10-in. -diam supply piping was connected to the RTF air supply system (Ref. 9), and a 4-in. long section of commercial stainless steel honeycomb was attached to the end of the 10-in. -diam piping and extended into a 30-in. -diam duct. The honeycomb was fabricated of 0.0028-in. thick stainless steel and contained 0.25-in. square cells (Fig. 13). Each cell had a length to width ratio of 16 in order that sufficient torque would be applied to the air stream as it flowed through the cell to remove any rotation of the flow. A flow straightening screen was installed approximately 9 plenum diameters downstream of the honeycomb to remove radial velocity variations in the flow. The 6-mesh screen with 0.041 wire was supported on a 6 by 6-in. grid (Fig. 14). Total blockage of the screen and support grid was 53 percent of the plenum area. The exit end of the 20-in. -diam duct was connected to the RTF exhaust system.

INSTRUMENTATION

Pressures and/or temperatures were measured at the stations shown in Fig. 12. Details of the instrumentation at each station are shown in Fig. 15.

The static pressure orifices at station 1 and in the traversing static pressure probe at station 2 were 0.040 in. in diameter; those at station 2

were 0.055 in. in diameter. (The desired orifice diameter at station 2 was 0.040 in., but a machining error resulted in the slightly oversized holes.) All orifices were hand-reamed to insure that they were sharp-edged and burr-free, and great care was exercised to insure that the surface surrounding the orifice was smooth and free of waves.

Details of the traversing static pressure probe used at station 2 are shown in Fig. 16. The probe was manually positioned at various radial positions in the venturi throat, and the probe position was determined from machined divisions in the probe support. The traversing total pressure probe (station 1) was a simple bent-tube probe, also manually positioned.

The boundary layer total pressure rake (Fig. 17a) used at station 2 was fabricated from 0.020-in. outside diameter by 0.005-in. wall thickness stainless steel hypodermic tubing, and the probe tips were unchamfered and not flattened. A view of the boundary layer rake installed in the venturi is shown in Fig. 17b. The distance of the probes from the venturi wall was measured with tapered feeler gages.

Single shielded, self-aspirating thermocouples were used at station 1 to measure the temperature of the air.

All pressures were measured on manometers and photographically recorded. Calibrated manometer fluids (mercury, tetrabromethane, and water) were used, and specific gravity corrections were applied to account for variations in fluid temperature.

Thermocouple outputs were measured with a manually balanced precision potentiometer.

PROCEDURE

Essentially dry air (moisture content approximately three grains per pound) was supplied to the venturi inlet (station 1) at a temperature of about 70°F and at the pressure required to produce the desired Reynolds number at the venturi throat. The pressure downstream of the venturi was maintained at the value required to produce the desired pressure drop across the venturi.

At each stabilized operating condition, several sets of data were recorded to provide a sufficiently large data sample to minimize the effect of random measurement errors on the average value of the parameters.

EXPERIMENTAL RESULTS

Venturi Inlet Flow

Both the honeycomb and the flow straightening screen (Figs. 12, 13, and 14) were installed upstream of the venturi to insure that the flow approaching the venturi was free of rotation and had a uniform velocity profile. Results of total pressure surveys made at station 1 (Fig. 18) indicated that within the measurement capability the total pressure was uniform across the stream.

Critical Operation of Venturi

To verify that critical flow conditions existed in the venturi, it was necessary to show that the throat conditions were independent of venturi overall pressure ratio for all pressure ratios greater than some limiting value. The total pressure in the throat boundary layer at the outermost probe position ($y = 0.010$ in.) and the average throat wall static pressure are shown in Fig. 19 as a function of overall venturi pressure ratio and of the position of the shock wave in the venturi. Boundary layer total pressure was independent of venturi pressure ratio above a value of about 1.2 (Fig. 19a). Throat wall static pressure (Fig. 19b) was independent of venturi pressure ratio above a value of 1.3 which corresponded to the shock wave location about 1.5 in. downstream of the throat (Fig. 19a). It is to be expected that pressure disturbances moving upstream through the subsonic boundary layer will affect the throat wall static pressure before the boundary layer total pressure is affected. Therefore, this venturi operates at critical flow conditions for all overall pressure ratios greater than 1.3.

However, it is possible to operate venturis at critical flow conditions at pressure ratios much less than the value of 1.3 indicated for this venturi. A large portion of the overall pressure drop occurred in the flow straightening screen located downstream of the venturi and in the sudden reduction in duct area located downstream of the screen (Fig. 12). Venturis of essentially identical configuration but exhausting into a plenum section have been operated in the RTF at critical flow conditions at overall pressure ratios of about 1.15.

Venturi Throat Boundary Layer

For all boundary layer total pressure data shown, the center-of-pressure of the probe was assumed to lie on the geometrical center of the probe (Ref. 10). The total pressure data presented here have not been corrected for normal shock wave losses for conditions at which the

data indicated that supersonic flow was approaching the probe; the maximum correction would be much less than 0.1 percent.

It was very difficult to determine precisely the distance of each boundary layer probe from the venturi wall. Therefore, to verify that the measurement technique was adequate, two different probe spacings were used. The excellent agreement of the boundary layer profiles (Fig. 20a) for the two probe spacings indicates that the distance measurements were satisfactory.

Throat boundary layer total pressure profiles for a range of venturi throat Reynolds numbers from 0.40×10^6 to 5.45×10^6 are shown in Figs. 20b and c. Three regimes of flow in the venturi boundary layer are clearly shown: (1) at the lowest values of Reynolds number ($0.40 \times 10^6 \leq Re \leq 0.68 \times 10^6$) the boundary layer was laminar up to the throat; (2) at the highest values of Reynolds number ($2.71 \times 10^6 \leq Re \leq 5.45 \times 10^6$) the boundary layer was turbulent for a large distance upstream of the throat so that a fully developed turbulent layer existed at the throat; and (3) in the range of Reynolds number between (1) and (2), the boundary layer transition from laminar to turbulent occurred sufficiently near the throat so that the boundary layer characteristics lay between the fully developed laminar and turbulent conditions.

The important comparison to be made is between the theoretical boundary layer values and the experimental values. Such a comparison of the theoretical and experimental boundary layer weight-velocity profiles is shown in Fig. 21 for two values of throat Reynolds number. The experimental values of weight-velocity are based on the measured values of boundary layer total pressure and venturi throat wall static pressure. Excellent agreement between the theoretical and experimental values at a Reynolds number of 5.45×10^6 is shown (Fig. 21b). At a Reynolds number of 1.33×10^6 the theoretical and experimental profile shapes are different (Fig. 21a) because of boundary layer transition effects; however, it can be seen that the integrated values of weight flow for the two profiles are very similar. For the purposes of this report, however, the most important comparison is that between the theoretical and experimental values of throat area reduction (Fig. 22). The experimental values of boundary layer displacement thickness required to compute the throat area reduction were determined by numerical integration of the measured weight-velocity profiles (e. g. Fig. 21). As can be determined from Fig. 22, the difference between the theoretical and experimental values is about 15 percent in the turbulent flow regime. This difference is very much less in the transitional regime, but the excellent agreement must be considered to be somewhat fortuitous.

It is very important to avoid the use of the boundary layer calculation method shown in Ref. 6 for the condition of laminar boundary layer throughout the contraction section. Therefore the value of Reynolds number at which boundary layer transition from laminar to turbulent flow will occur must be determined. The problem of boundary layer transition on a convex surface has been investigated by Liepmann (Ref. 11). His results show that a boundary layer transition from laminar to turbulent flow occurs on a convex surface at a Reynolds number (based on boundary layer momentum thickness, θ) of 1000. According to this criterion, transition should occur at the venturi throat for the specific configuration used in this investigation at a value of Re just slightly greater than 0.68×10^6 , and this value agrees with the values obtained in this investigation, based on the behavior of throat area reduction (Fig. 22). Thus, an adequate criterion appears to exist which will define the minimum Reynolds number at which the method of Ref. 6 is applicable.

Venturi Throat Weight-Velocity Gradients

Mach number profiles across the venturi throat are shown in Fig. 23a for a range of Reynolds number at critical flow conditions. The corresponding weight-velocity profiles based on isentropic flow (constant total pressure) from the inlet plenum (station 1) are shown in Fig. 23b. The validity of the assumption of constant total pressure between stations 1 and 2 in the flow region which is not affected by viscous effects is verified in Fig. 20 since the measured total pressure in the throat became equal to the plenum pressure a very short distance from the venturi wall.

No variation in centrifugal force field effects was expected as a function of viscous effects or Reynolds number, and the experimental results (Fig. 23) show no variation of throat conditions as a function of Reynolds number.

The theoretical variation of conditions across the venturi throat are also shown in Fig. 23; excellent agreement exists between the theoretical and experimental values. A numerical integration of the results shown in Fig. 23b gives a value of 0.9985 for the ratio of actual flow rate to the one-dimensional value, and this value of 0.9985 compares with the value of 0.9980 obtained from theoretical considerations (see Theoretical Determination of Venturi Discharge Coefficient).

One unexpected result obtained was the small but systematic variation of venturi throat wall static pressure, p_{2w} , [hence Mach number based on p_{2w} (Fig. 23a)] at critical flow conditions as a function of Reynolds number. The reason for this variation is not known, but it

must be related to the fact that the actual flow curvature very near the wall is a function not only of the wall curvature, but also of the boundary layer displacement thickness. Another possible explanation might relate to the effect of Reynolds number on the pressure indicated by a static orifice (e. g. see Ref. 12), but this explanation is unlikely because a similar effect would also have been shown by the trailing static pressure probe measurement, P_{2f} , and hence M_{2f} .

COMPARISON OF THEORETICAL AND EXPERIMENTAL VALUES OF VENTURI DISCHARGE COEFFICIENT

By combining the measured effects of boundary layer displacement thickness (Fig. 22) and centrifugal forces (Fig. 23b) on the flow at the venturi throat, the discharge coefficient for the venturi can be obtained. Both the experimental and the theoretical discharge coefficients for the critical flow venturi used in this investigation are shown in Fig. 24 as a function of Reynolds number. The theoretical approach for the determination of venturi discharge coefficients outlined in this report yielded values of coefficients which agreed with the experimental values within ± 0.06 percent.

LIMITATIONS OF METHOD

Several limitations must be applied to the theoretical method presented in this report for determining the discharge coefficient of venturis operating at critical flow conditions.

The most important limitation is that the venturi contour must be designed so that the boundary layer and centrifugal force field effects are small and, therefore, the theoretical discharge coefficient will be near unity (greater than 0.99). This does not represent a severe limitation, however, because this high value of coefficient is obtained with a simple venturi contour.

The venturi contour selected must also insure well behaved flow at all points upstream of the throat area and for a small distance aft of the throat to insure maximum reliability of the theoretical values. Basically regions having small favorable pressure gradients or, even worse, adverse pressure gradients (diffusing flow) must not exist because such conditions introduce large uncertainties in the theoretical boundary layer values. Discontinuous changes in wall curvature near the throat must be avoided because shock waves with attendant boundary layer thickening and/or flow separation may be encountered.

This theoretical method is restricted to venturis which operate in the turbulent flow regime. Thus the venturi operating conditions and physical dimensions must be selected so that the Reynolds number is sufficiently high to cause the transition from laminar to turbulent boundary layer to occur very near the leading edge of the venturi contraction section.

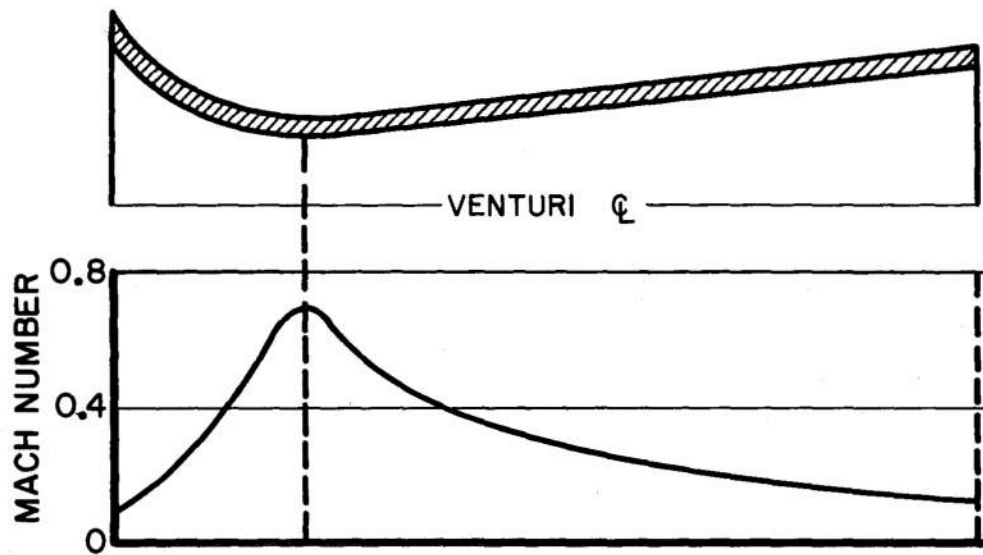
CONCLUSIONS

The following conclusions may be drawn concerning a theoretical method for determining the discharge coefficients for venturis operating at critical flow conditions.

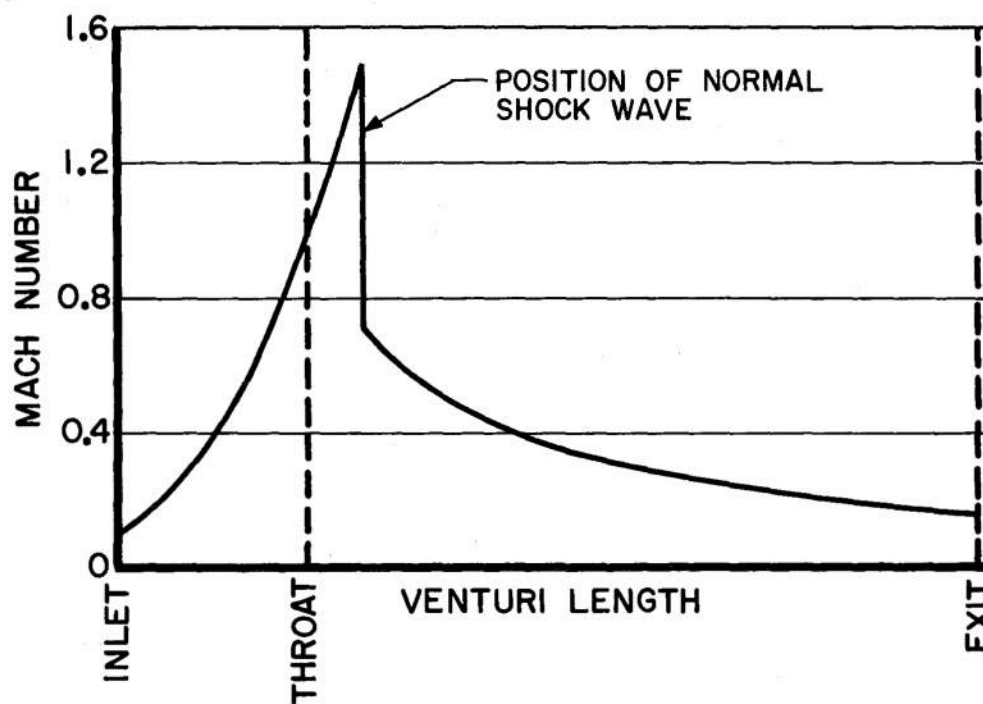
1. The discharge coefficient for a specially designed venturi operating at critical flow conditions can be calculated using long accepted theoretical aerodynamic techniques to within ± 0.06 percent of the experimental values. This coefficient considers the non-isentropic and non-one-dimensional flow effects which exist in the flow of a real gas and relates the flow rate of a real gas to the flow rate for the one-dimensional isentropic steady flow of a perfect gas at critical velocity.
2. A simple venturi contour consisting of a circular arc contraction section which extends up to and beyond the throat and is faired into a conical diverging section is most suitable for use at critical flow conditions because it provides an aerodynamic model for which reliable calculations of flow conditions at the throat can be made.
3. Presently recommended standard nozzle and venturi shapes are undesirable for use at critical flow conditions because of a continuously varying wall curvature in the contraction section, a discontinuous wall curvature near the throat region, and a cylindrical throat. These factors preclude the possibility of accurately determining the discharge coefficient by theoretical means. In general, experimental facilities for calibration of large venturis at critical flow conditions do not exist.
4. Venturis can be operated at critical flow conditions with low values of overall pressure ratio of approximately 1.15. This value of pressure ratio is not significantly different from the values required for operation of orifices and simple nozzles at subsonic conditions.

REFERENCES

1. Cope, W. F. "The Absolute Measurement of Rate of Flow of Large Quantities of Gas." British Aeronautical Research Council Report No. ARC 17, 691, June 1955.
2. American Society of Mechanical Engineers. Supplement to Power Test Codes, "Chapter 4: Flow Measurement Part 5 - Measurement of Quantity of Materials." ASME, PTC 19.5, April 1959.
3. Shapiro, A. H. The Dynamics and Thermodynamics of Compressible Fluid Flow. The Ronald Press Company, New York, 1953.
4. Patterson, G. N. "Modern Diffuser Design." Aircraft Engineering, Vol. X, No. 115, September 1938, pp 267-273.
5. Liepmann, H. W. and Roshko, A. Elements of Gasdynamics. John Wiley and Sons, Inc., New York, 1957, p 306.
6. Tucker, M. "Approximate Calculation of Turbulent Boundary-Layer Development in Compressible Flow." NACA TN 2337, April 1951.
7. Oswatitsch, K. and Rothstein, W. "Flow Pattern in a Converging-Diverging Nozzle." NACA TM 1215, March 1949.
8. Sauer, R. "General Characteristics of the Flow Through Nozzles at Near Critical Speeds." NACA TM 1147, June 1947.
9. Test Facilities Handbook, (3rd Edition). "Rocket Test Facility, Vol. 2." Arnold Engineering Development Center, January 1961.
10. Davies, P.O.A.L. "The Behavior of a Pitot Tube in Transverse Shear." British Aeronautical Research Council Report No. ARC 19, 709, December 1957.
11. Liepmann, H. W. "Investigation of Boundary Layer Transition on Concave Walls." NACA ACR 4J28, February 1945.
12. Shaw, R. "The Measurement of Static Pressure." British Aeronautical Research Council Report No. ARC 20, 829, March 1959.



a. Typical Subcritical Flow Conditions



b. Typical Critical Flow Conditions

Fig. 1 Ideal Mach Number Distribution along Venturi Length at Typical Subcritical and Critical Flow Conditions

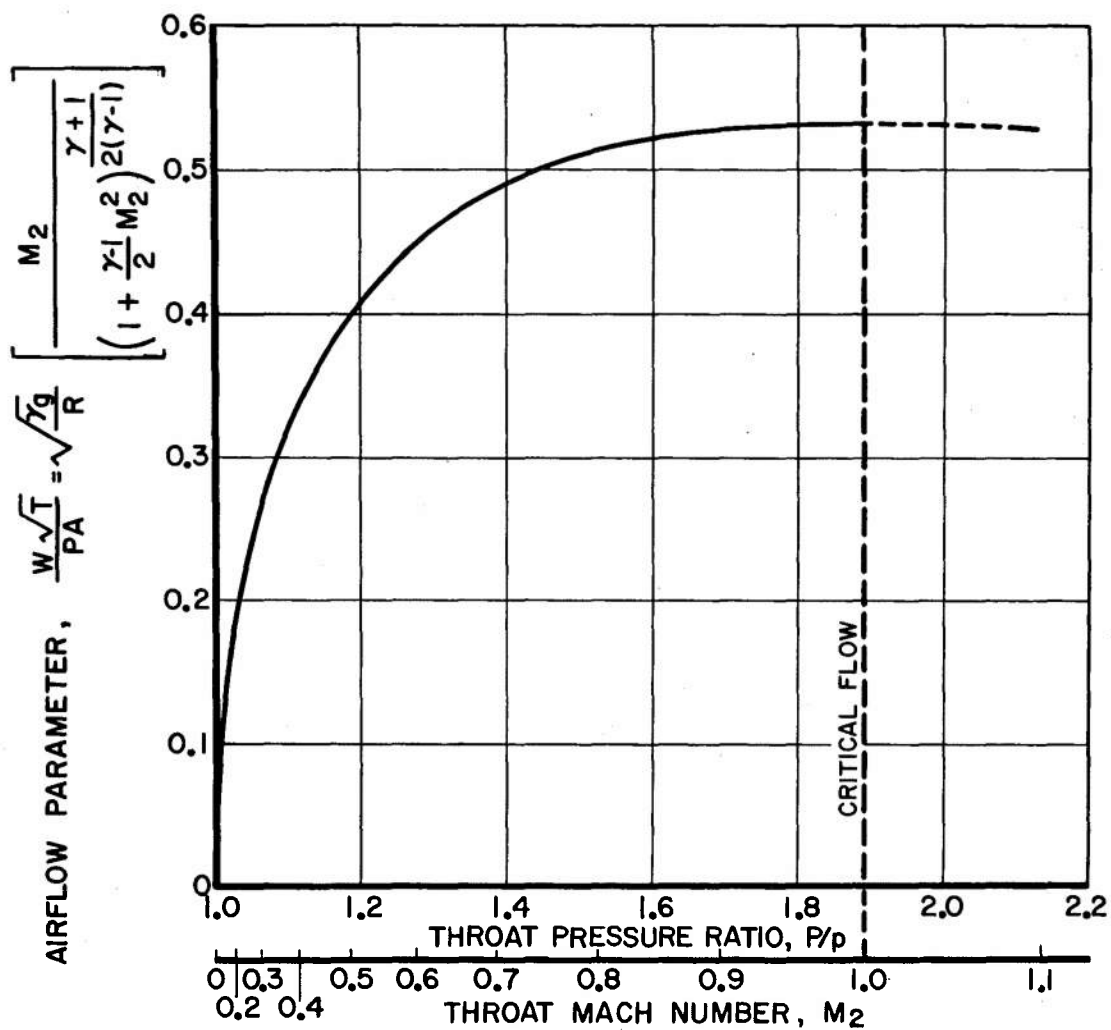


Fig. 2 Ideal Weight Flow per Unit Area at Venturi Throat as a Function of Throat Pressure Ratio and Mach Number: Air, $\gamma = 1.40$

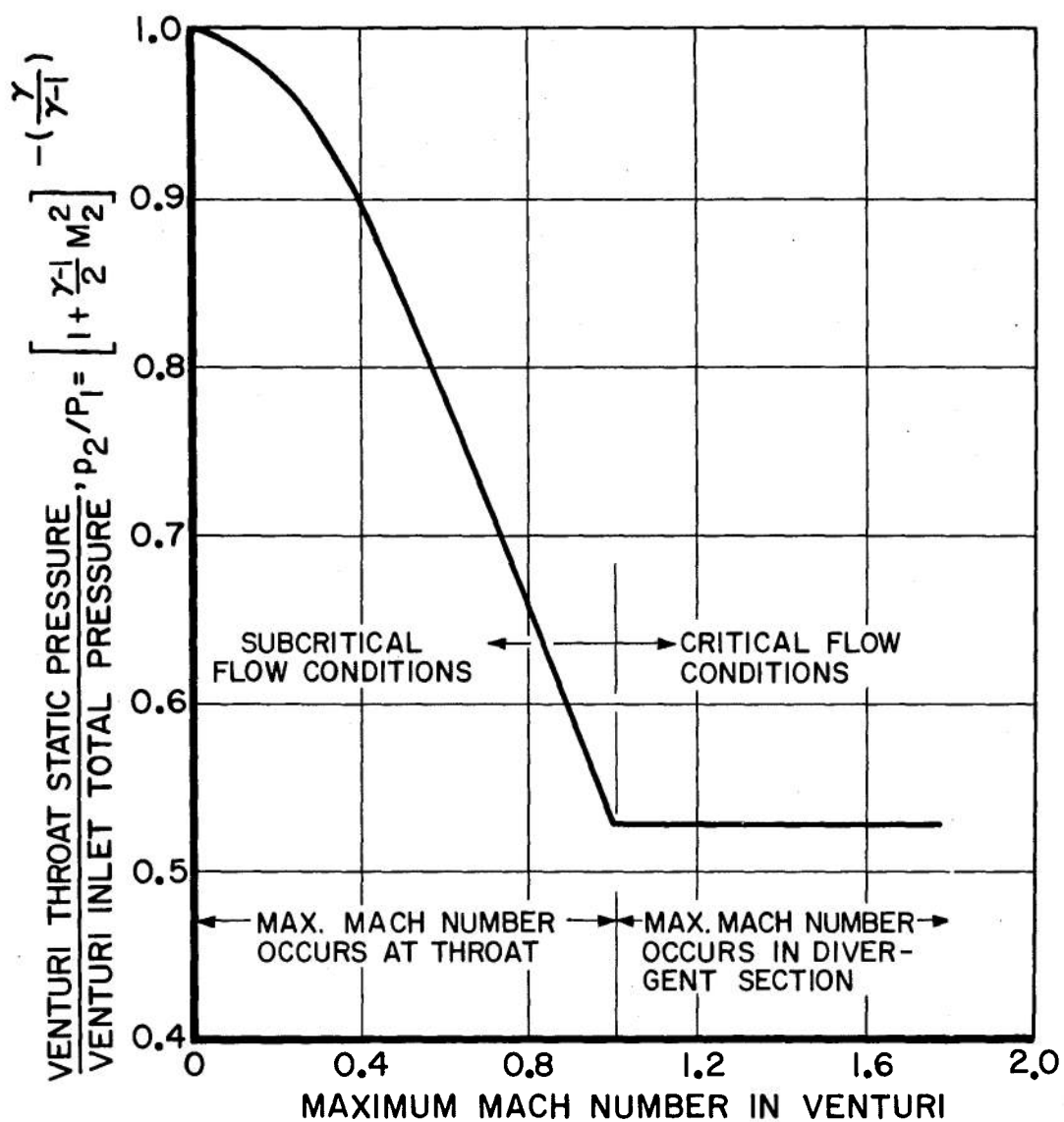


Fig. 3 Variation of Ideal Venturi Throat Static Pressure with Maximum Mach Number in Venturi: $\gamma = 1.40$

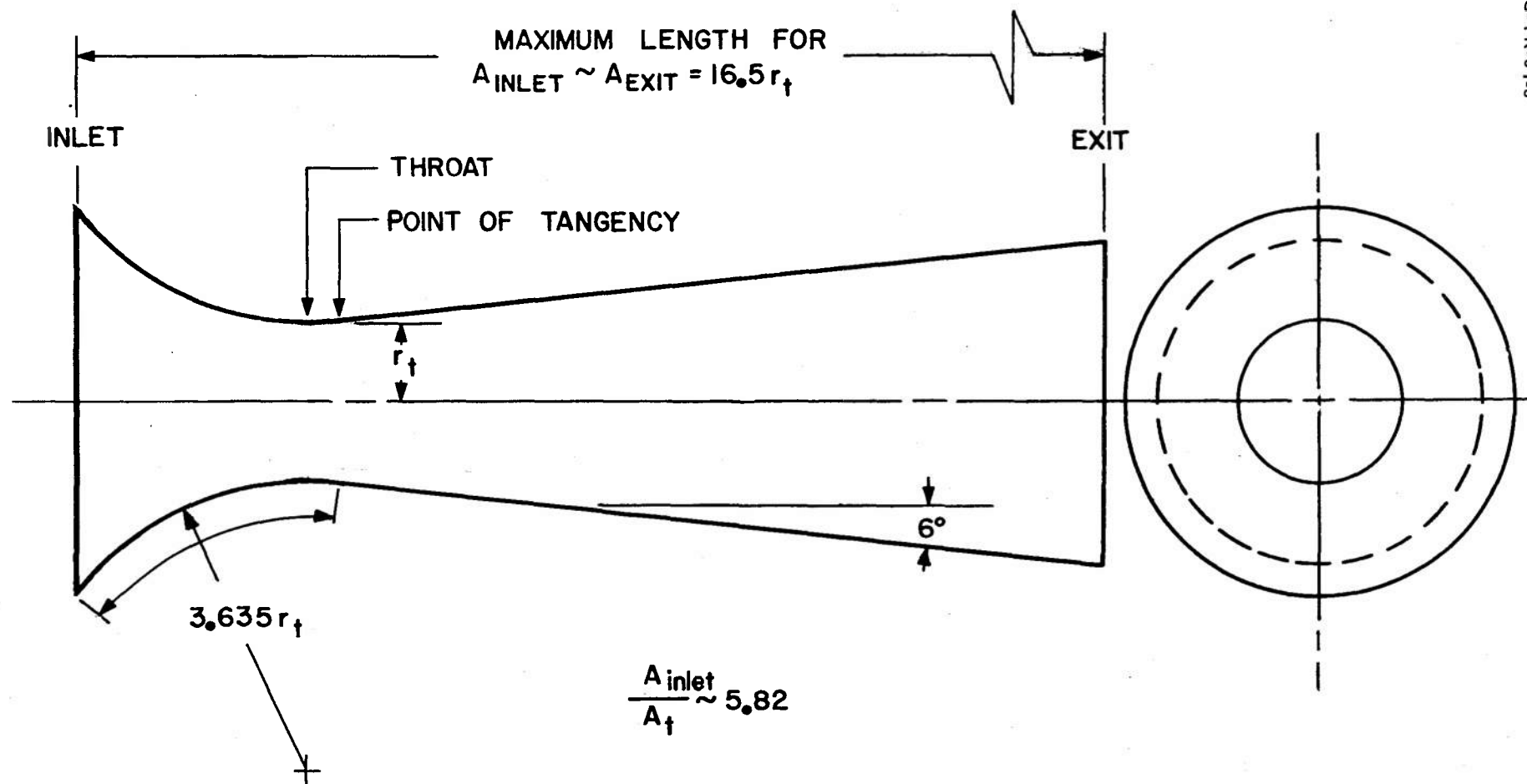
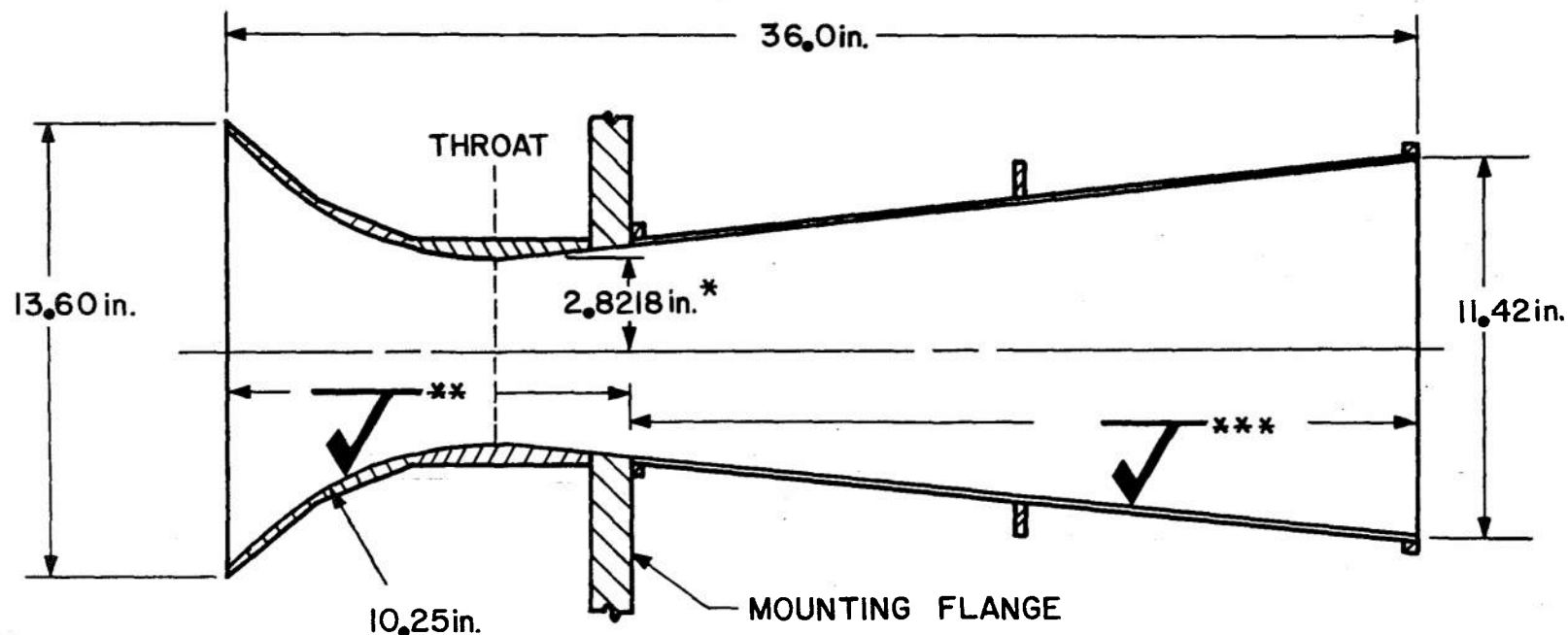


Fig. 4 Schematic of Venturi Design for Operation at Critical Flow Conditions



MATERIAL: MILD STEEL

* ALL DIMENSIONS SHOWN EXCEPT THROAT RADIUS ARE NOMINAL VALUES. THROAT RADIUS IS A PRECISION "AS-BUILT" VALUE.

** MACHINED SURFACE PAINTED. SURFACE FINISH OVER PAINT 30-50 MICRONS.

*** ROLLED STEEL SHEET AND PAINTED AS ABOVE.

a. Section Through Venturi

Fig. 5 Details of Venturi Used for Investigation



b. Right Front View

Fig. 5 Concluded

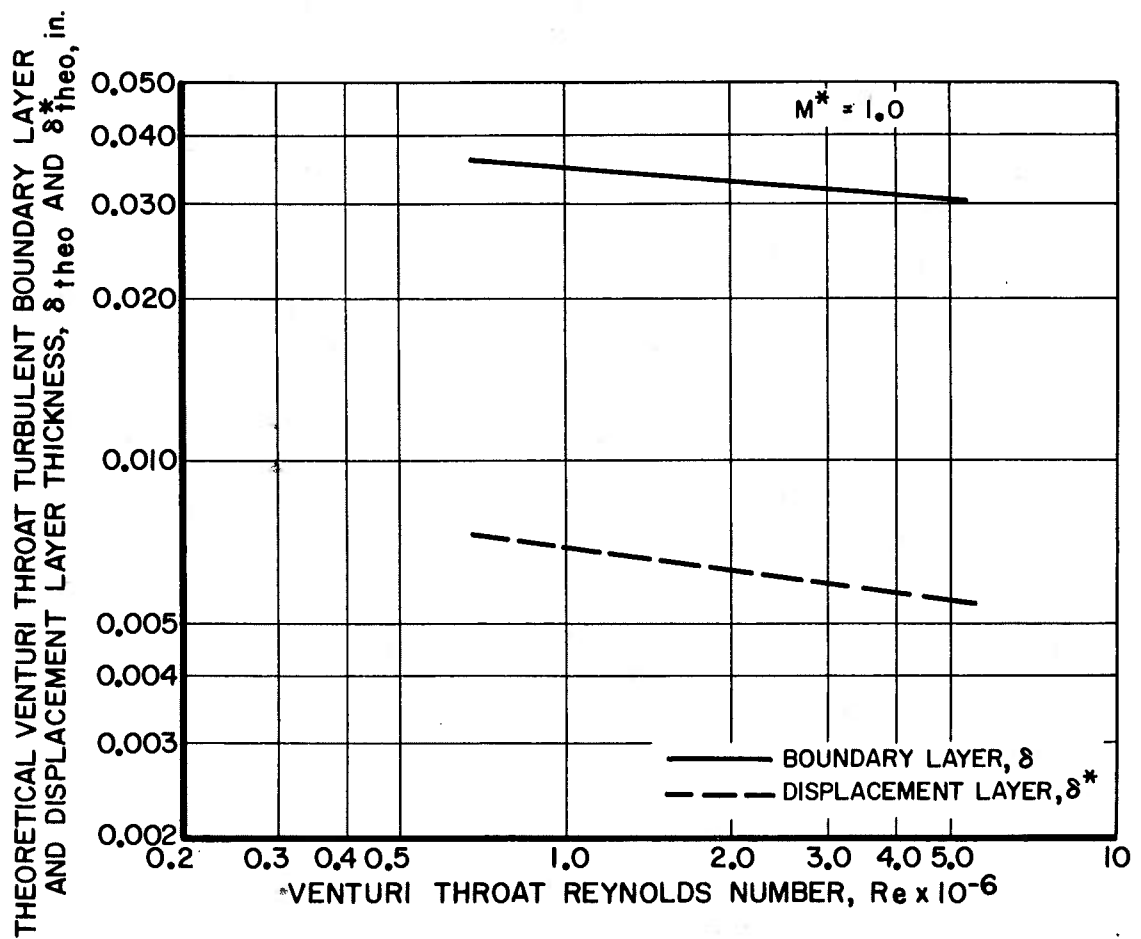


Fig. 6 Theoretical Values of Venturi Throat Turbulent Boundary Layer and Displacement Layer Thickness

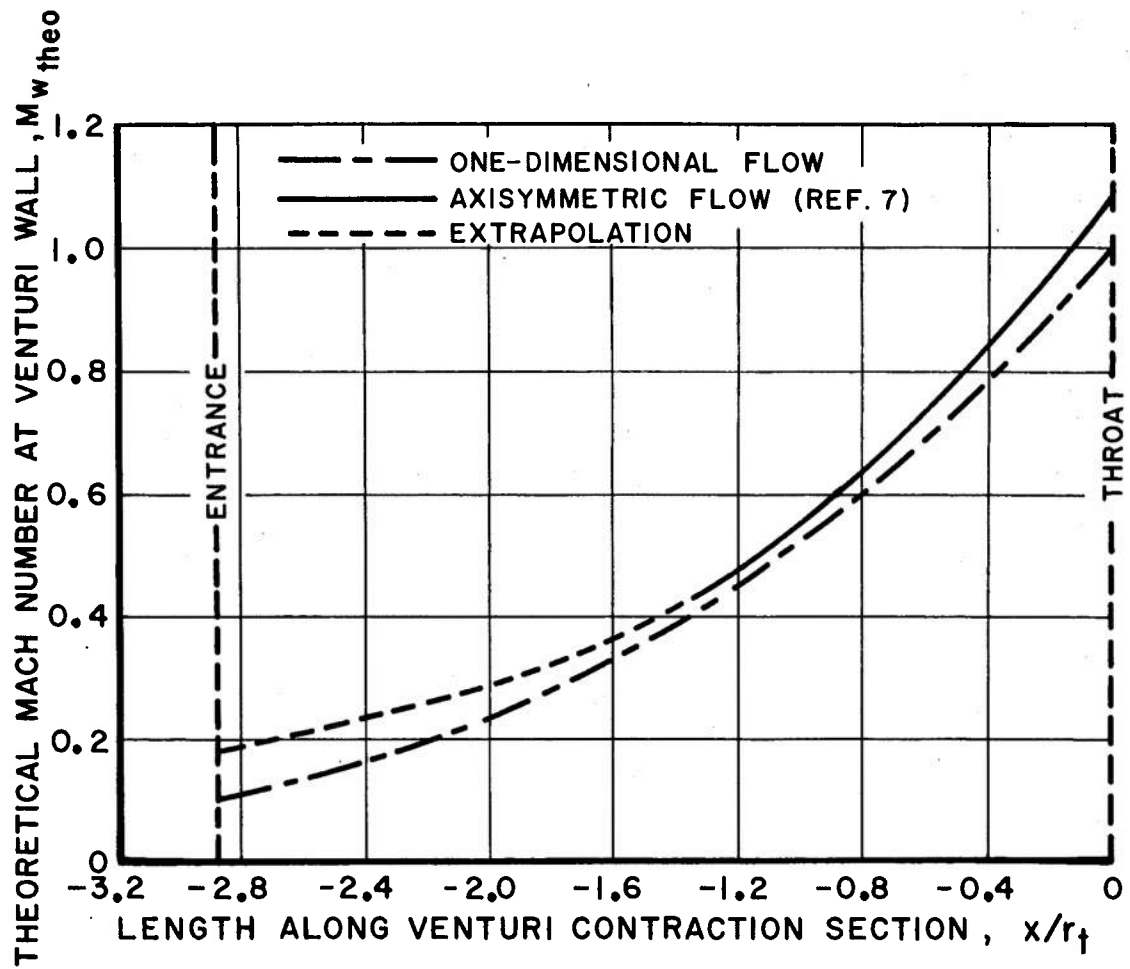
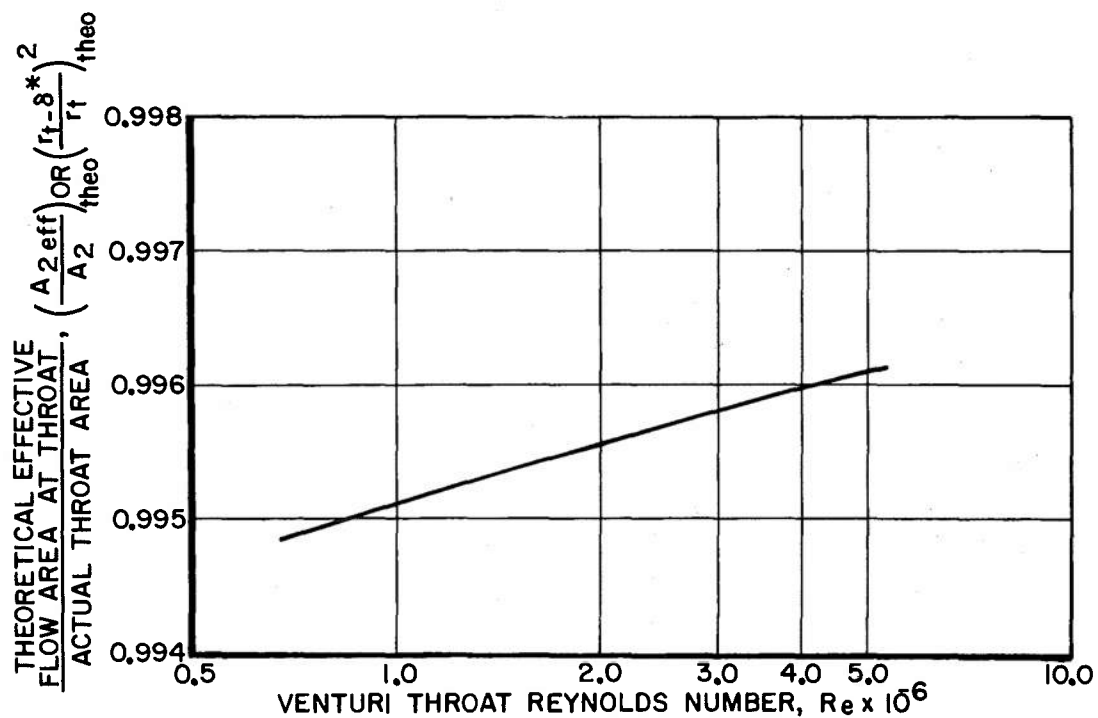
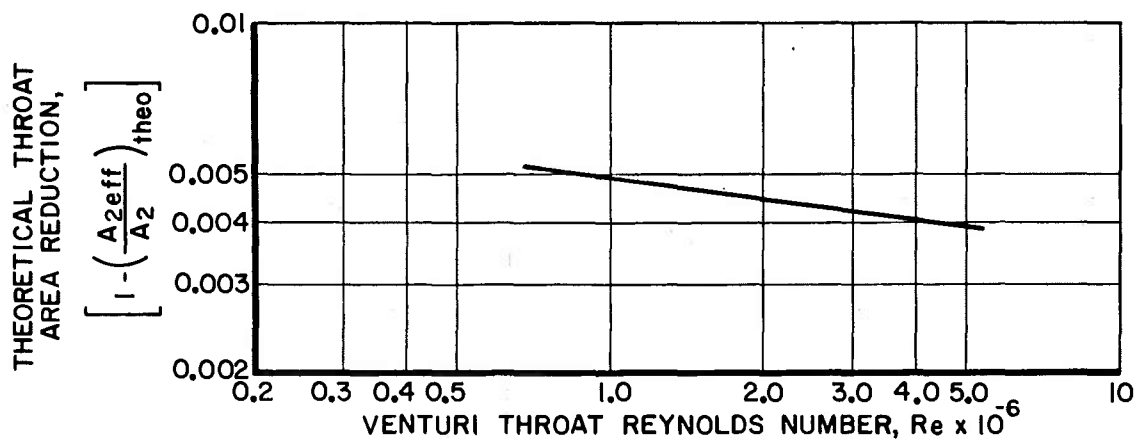


Fig. 7 Theoretical Mach Number Distribution along Venturi Wall for One-Dimensional and Axisymmetric Flow



a. Effective Throat Area



b. Throat Area Reduction

Fig. 8 Effect of Theoretical Values of Displacement Layer Thickness on Effective Flow Area at Venturi Throat

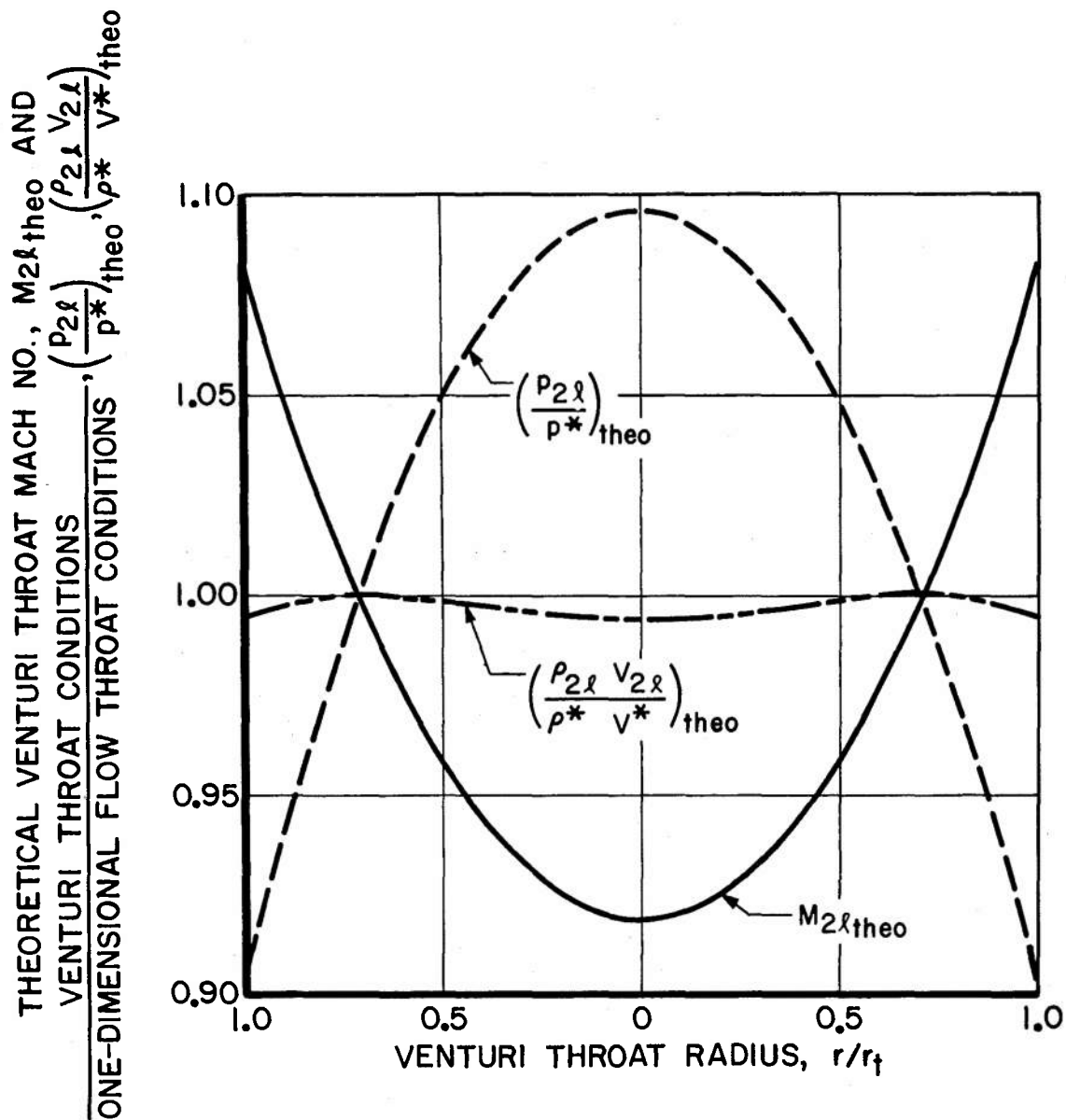


Fig. 9 Theoretical Variation of Mach Number, Static Pressure, and Weight-Velocity across Venturi Throat

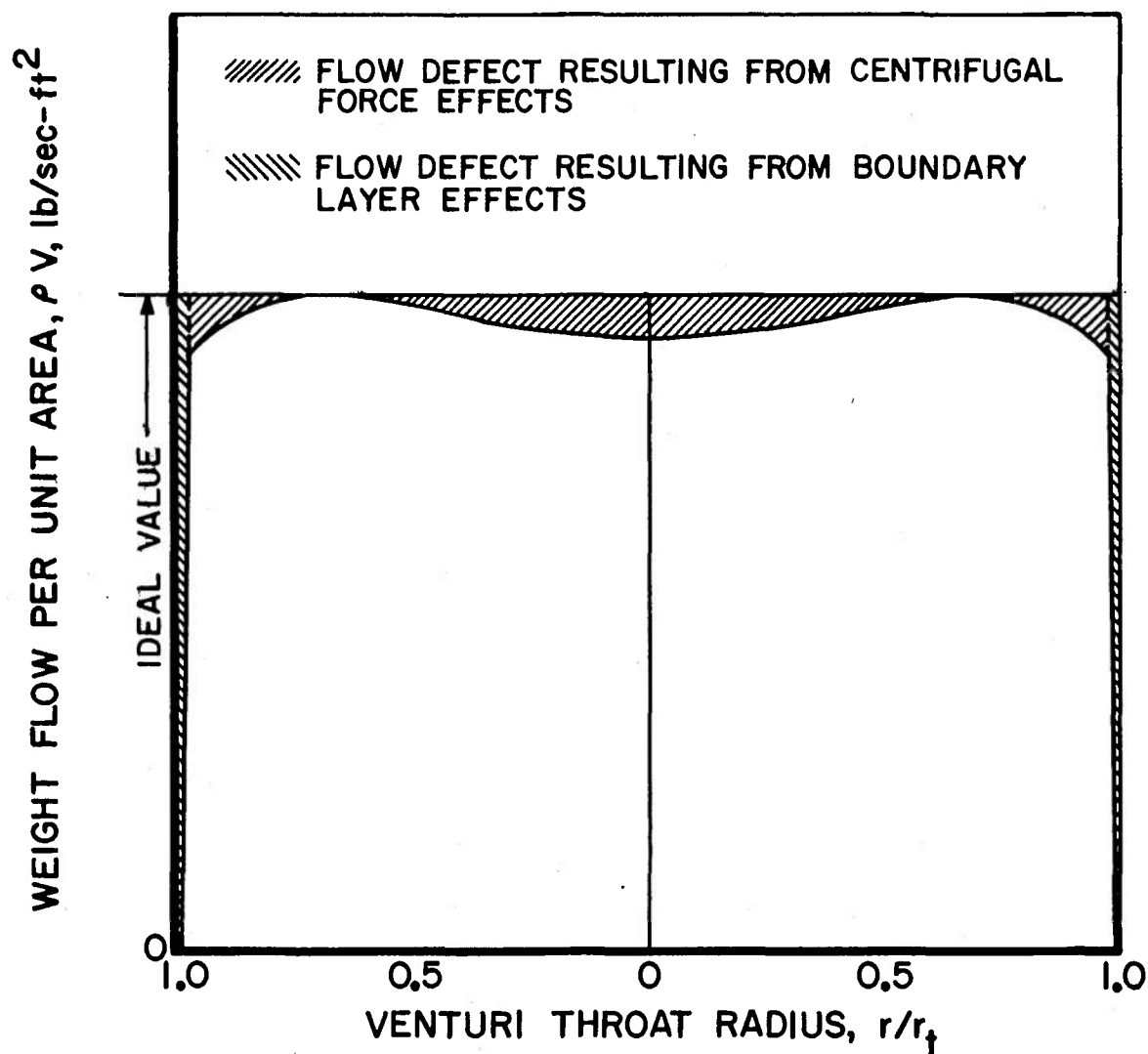


Fig. 10 Schematic Representation of Flow Defects at Venturi Throat

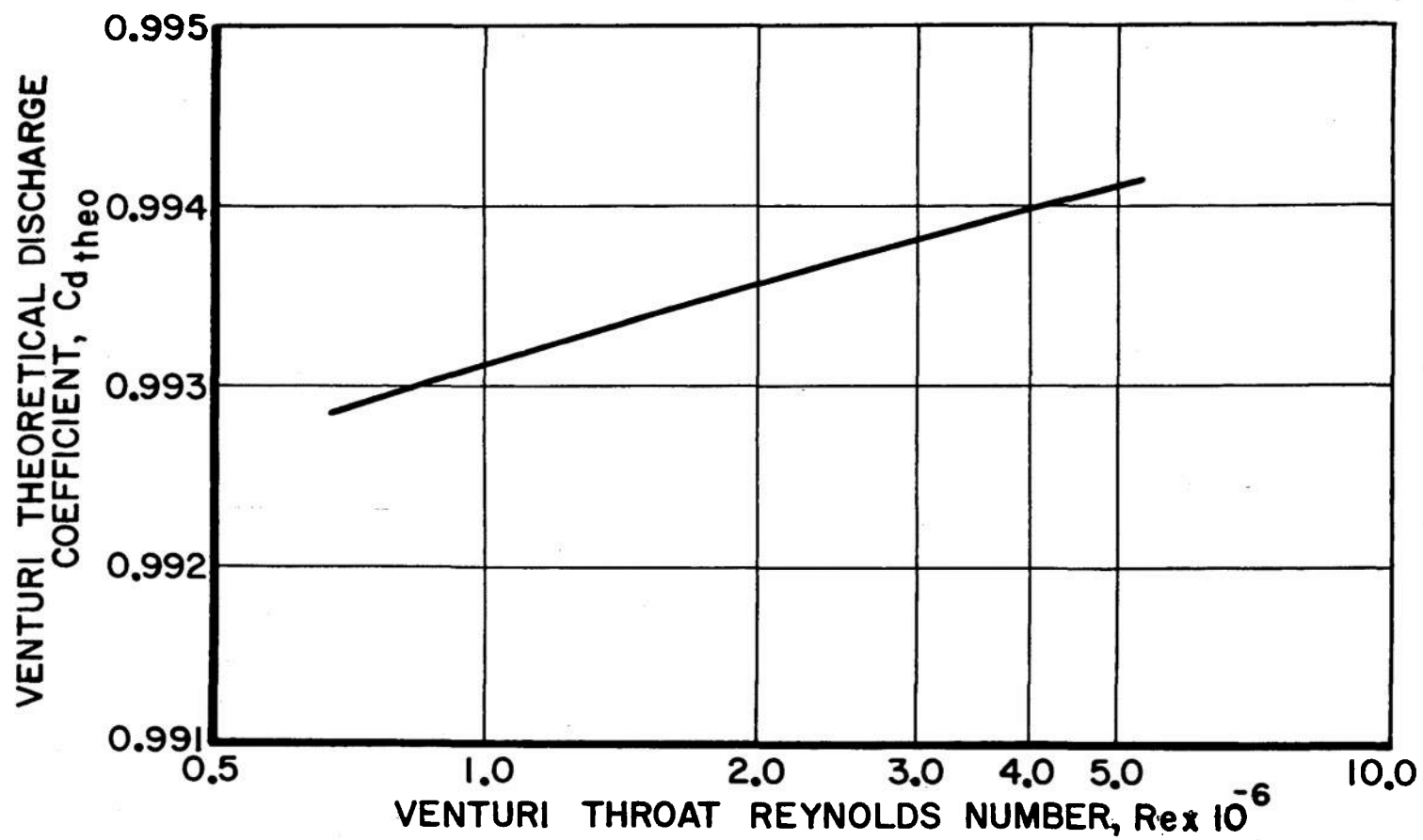


Fig. 11 Theoretical Values of Venturi Discharge Coefficient

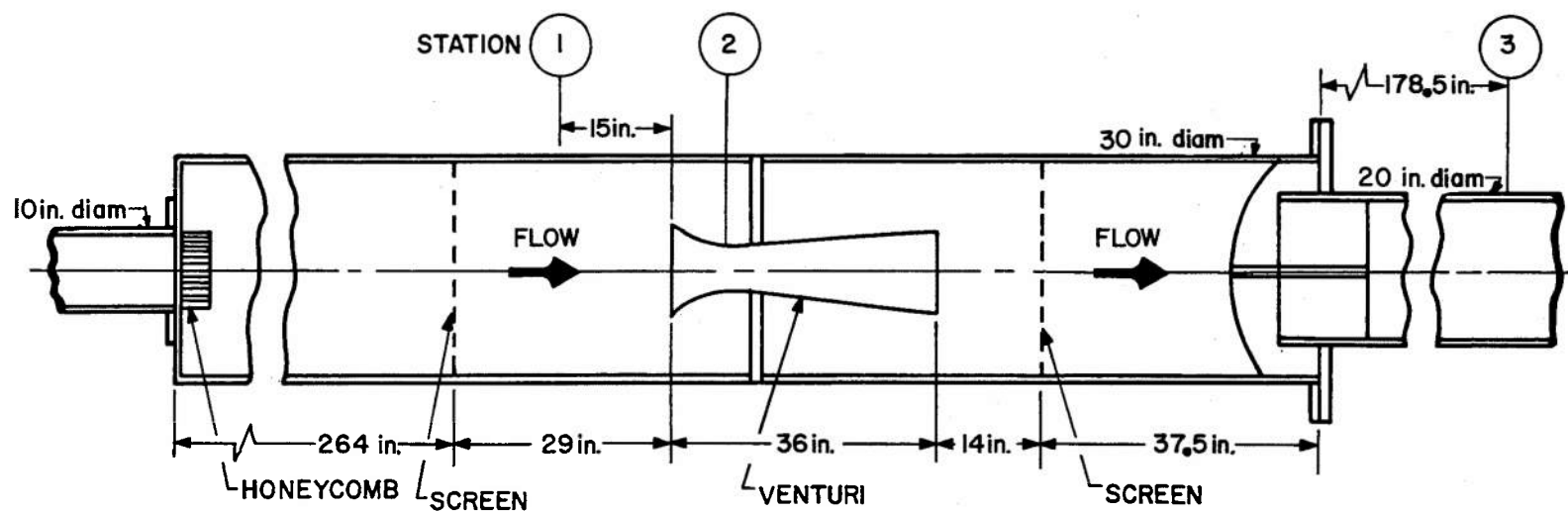


Fig. 12 Venturi Installation

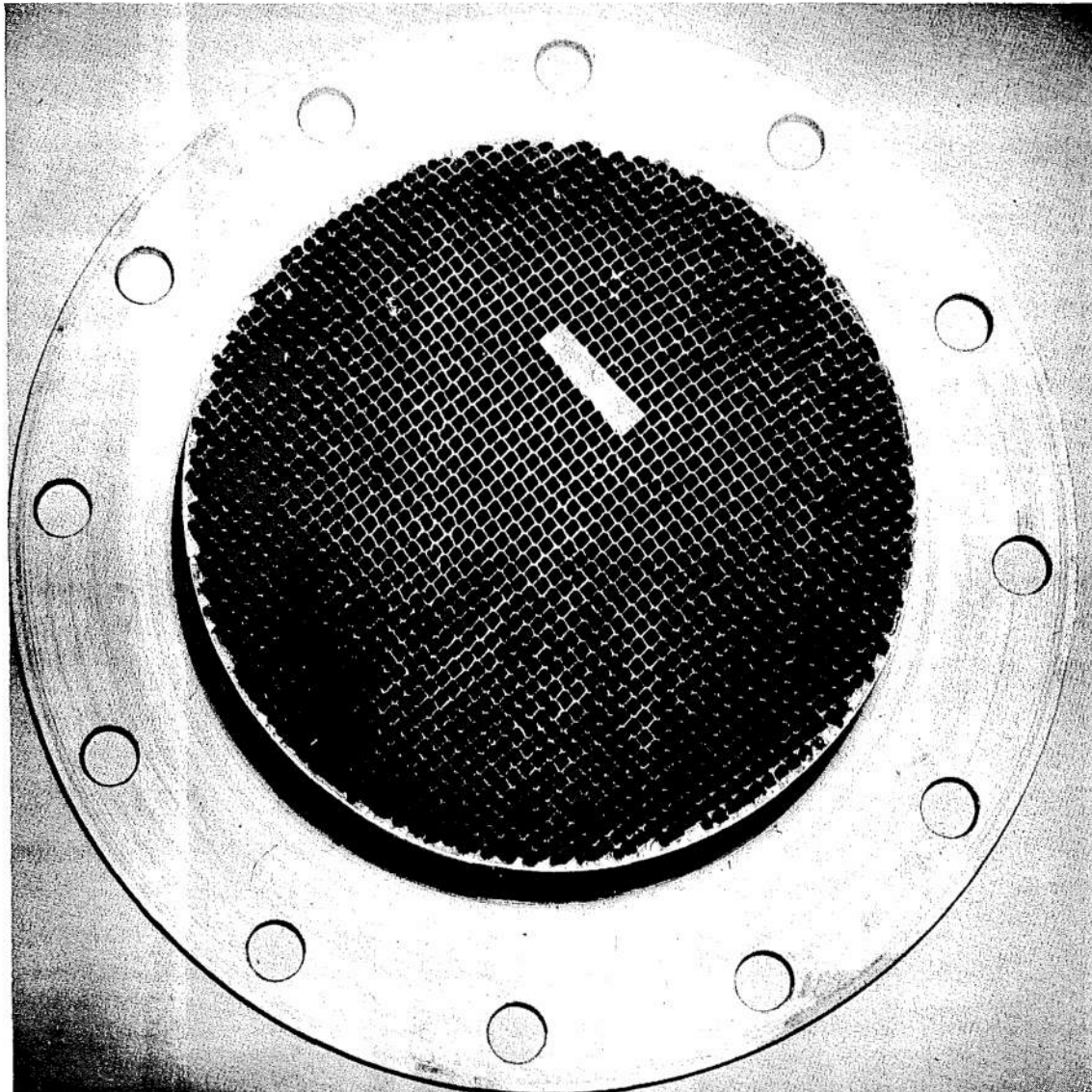


Fig. 13 View of Downstream End of Honeycomb Assembly

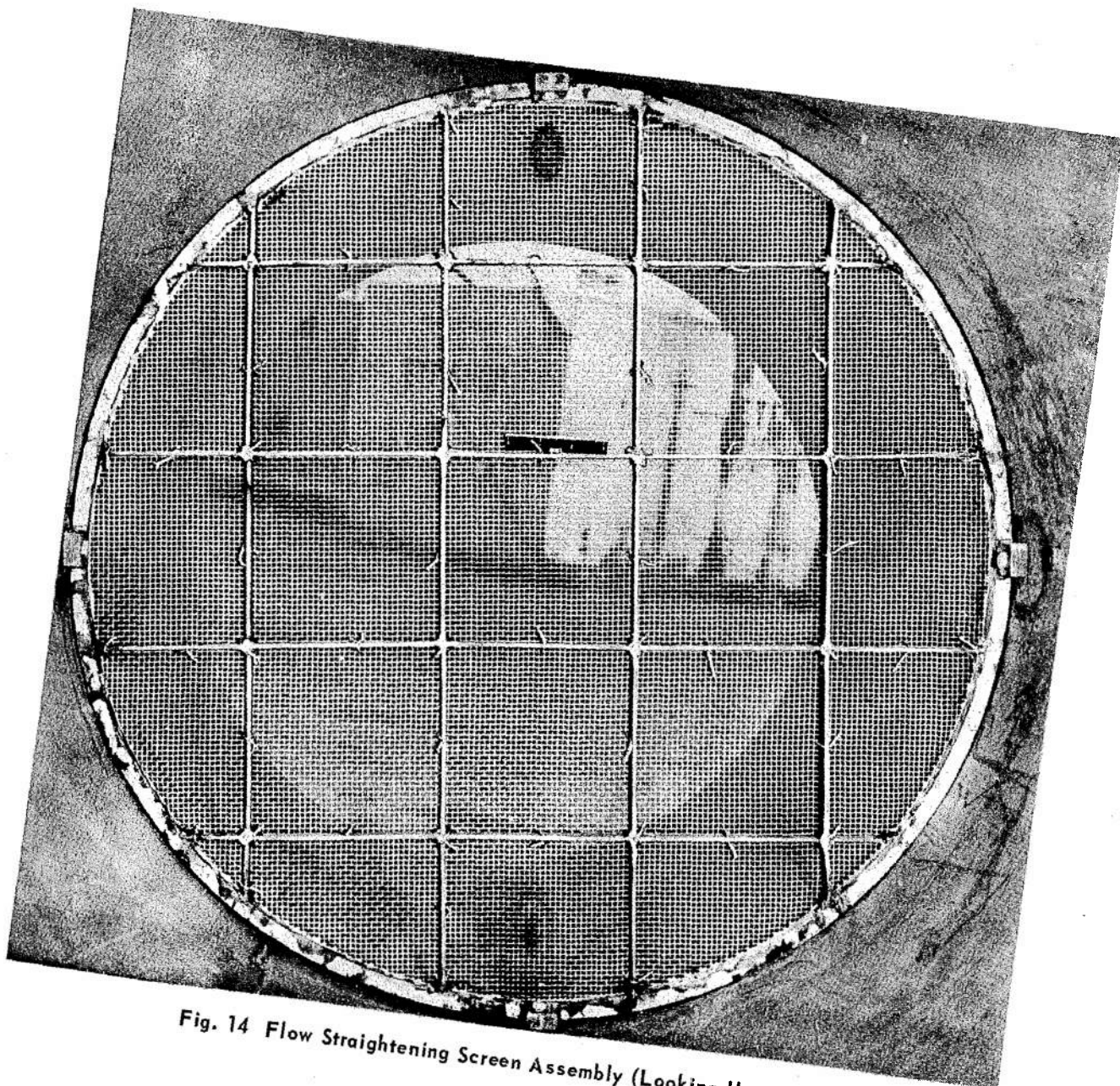


Fig. 14 Flow Straightening Screen Assembly (Looking Upstream)

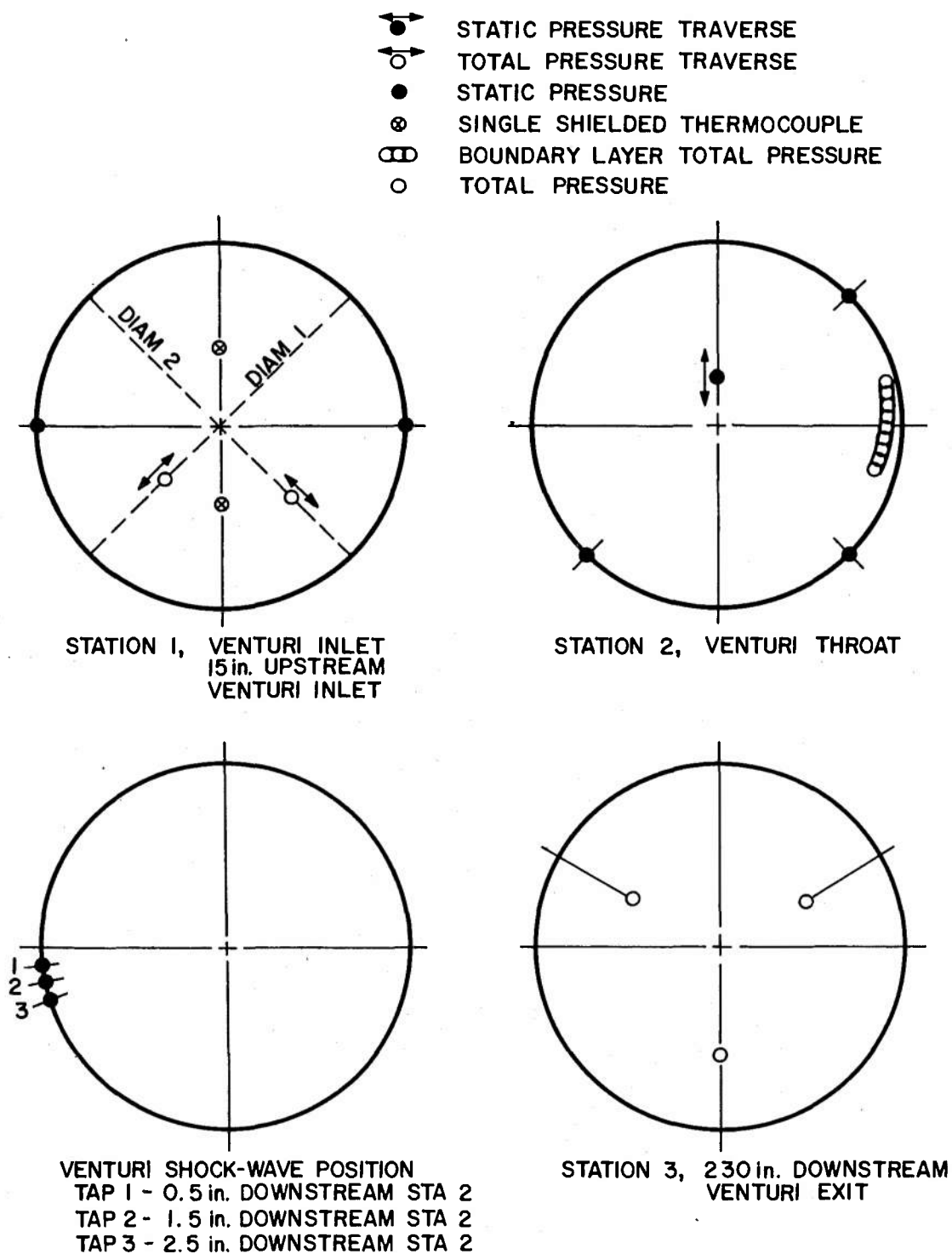


Fig. 15 Instrumentation Locations (Looking Upstream)

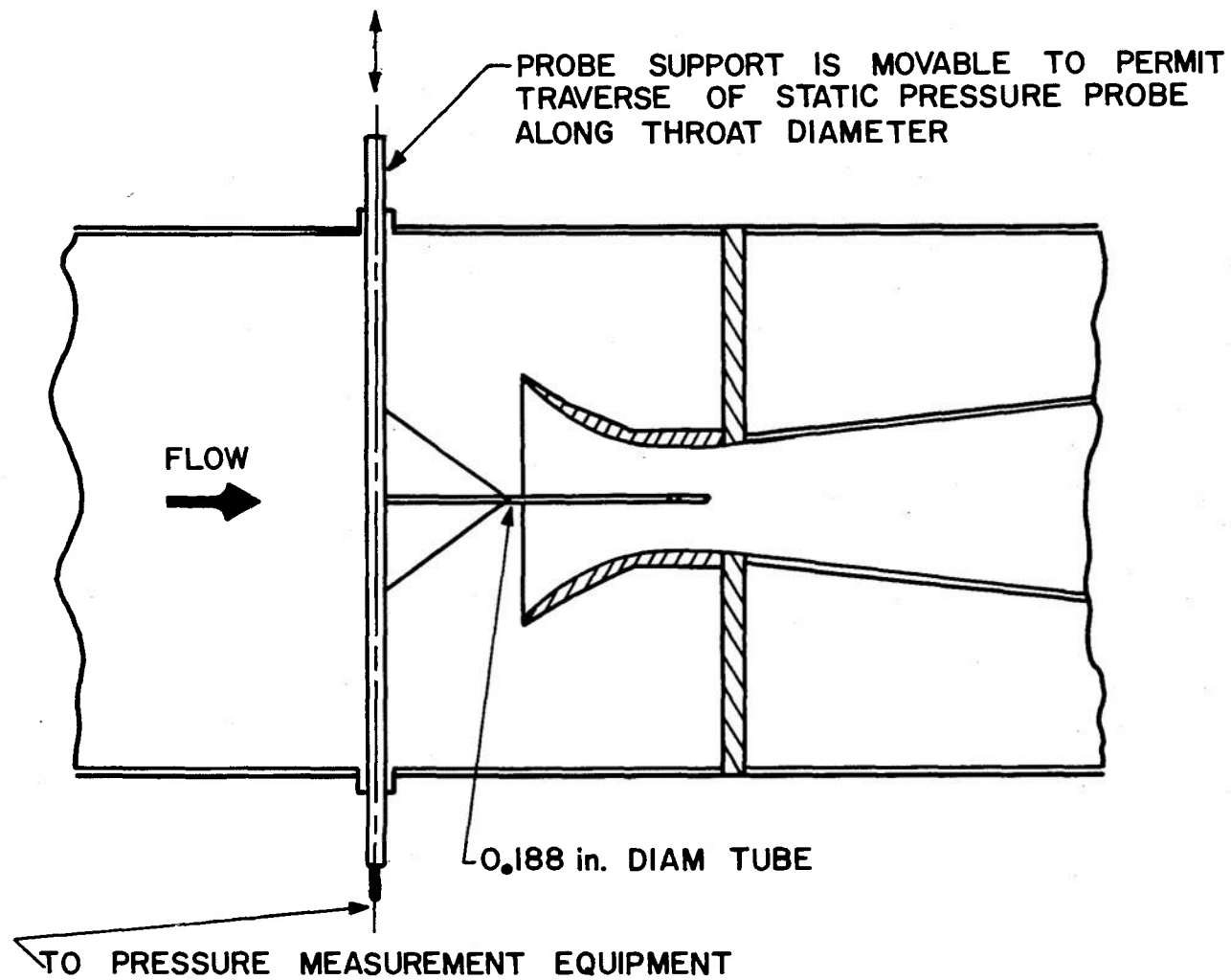
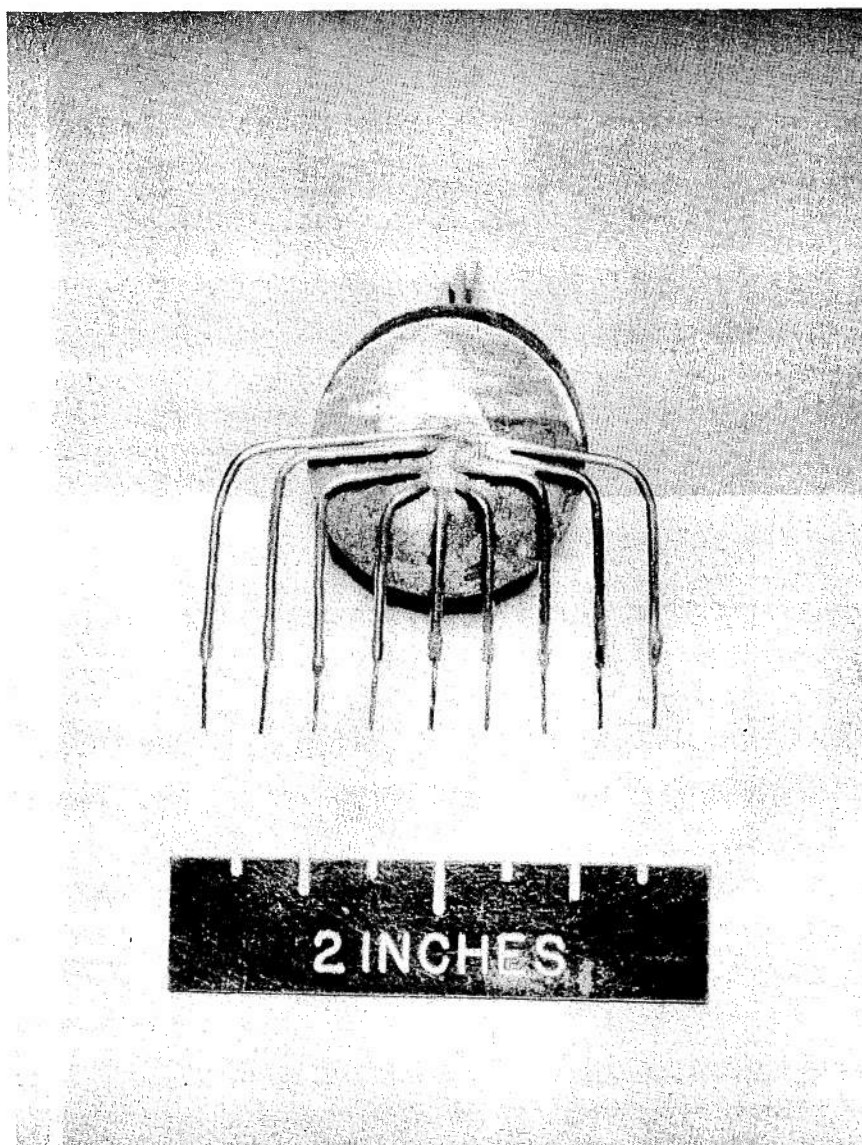
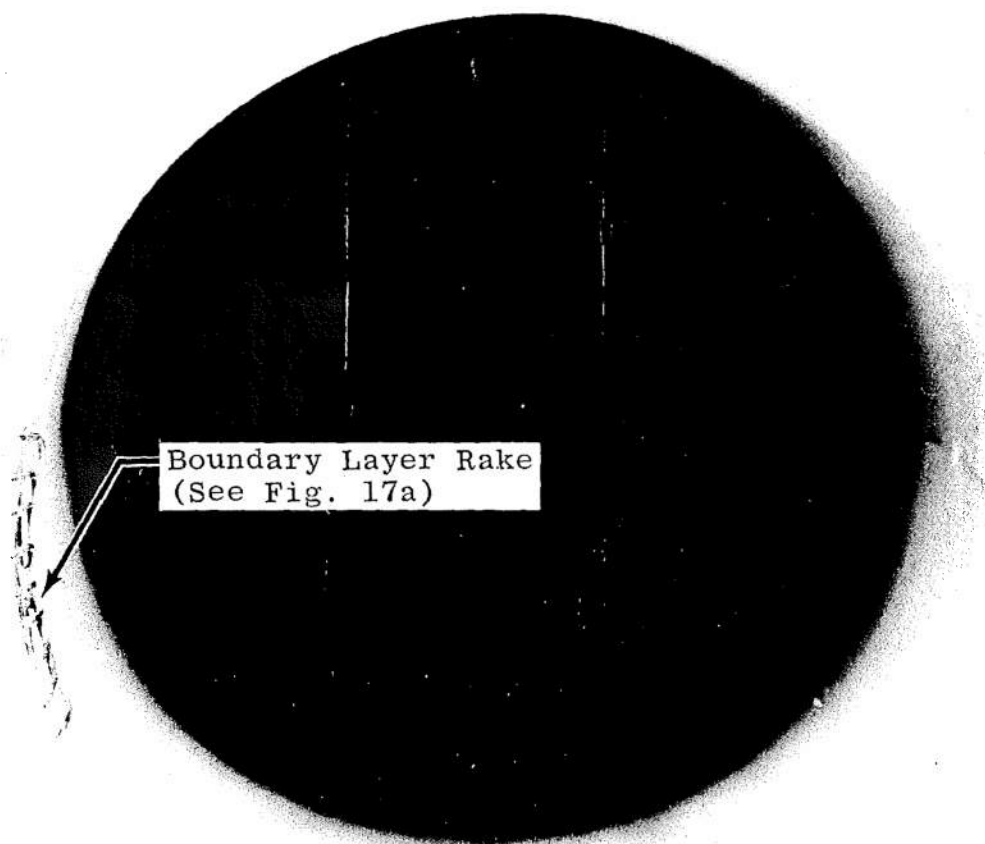


Fig. 16 Traversing Static Pressure Probe at Venturi Throat



a. Rake Top View

Fig. 17 Boundary Layer Rake



Boundary Layer Rake
(See Fig. 17a)

b. Installed in Venturi Throat (Looking Downstream)

Fig. 17 Concluded

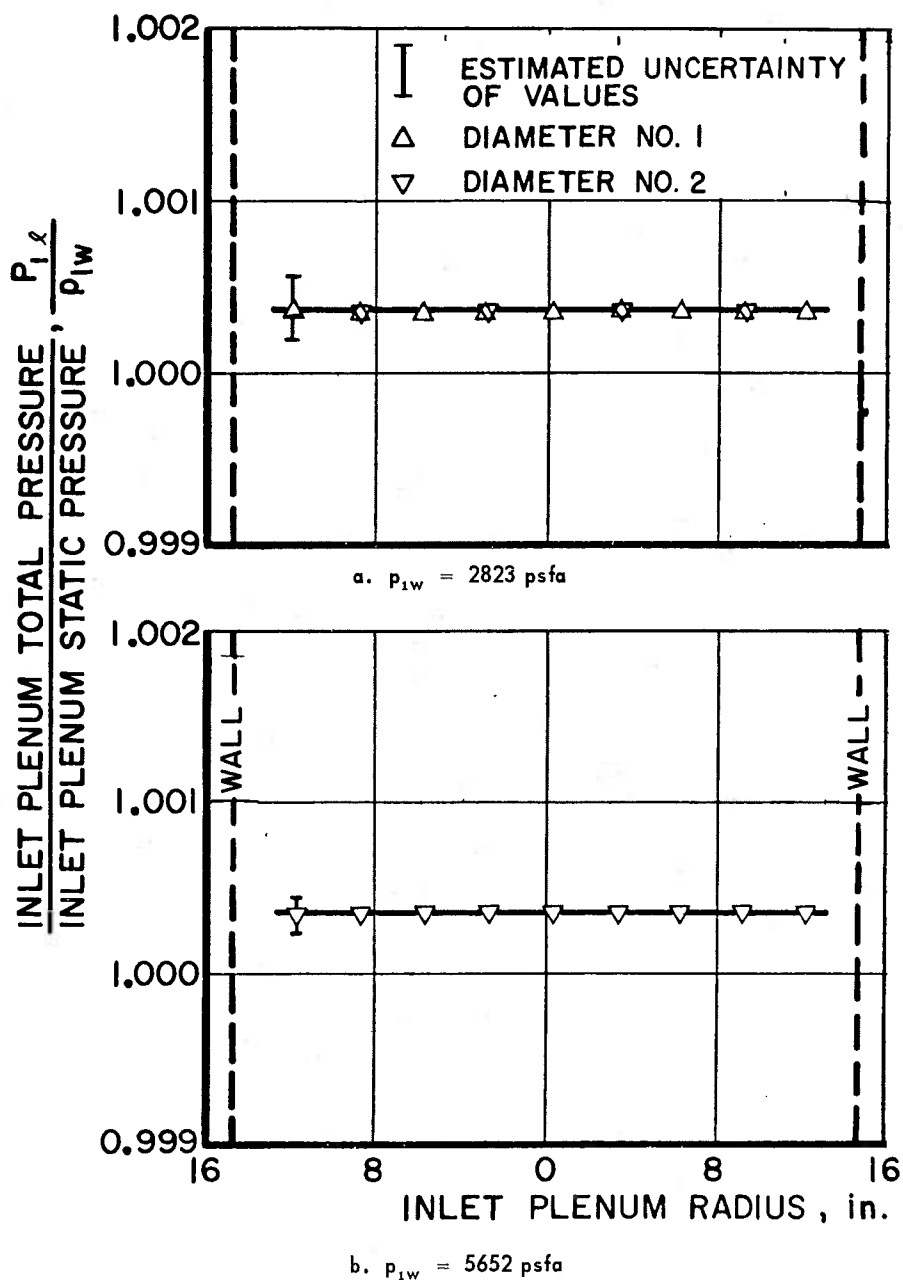
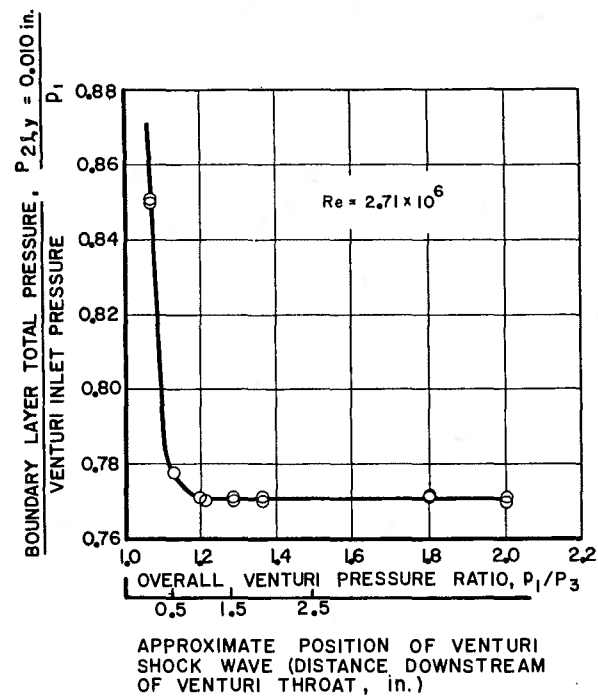
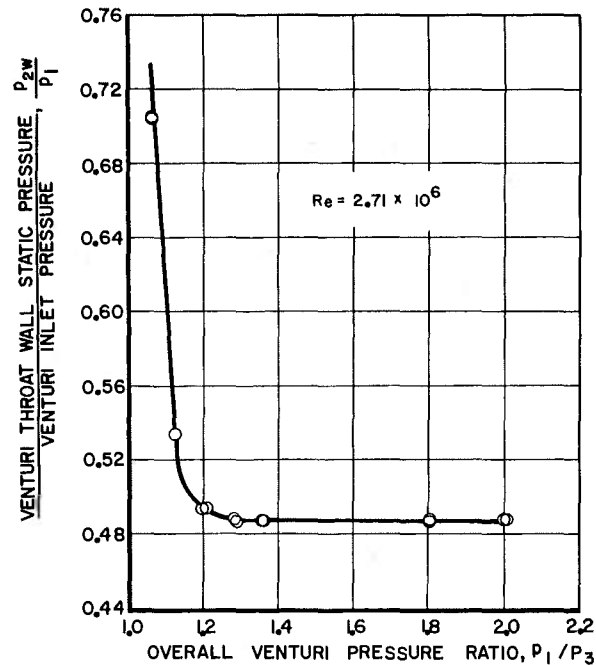
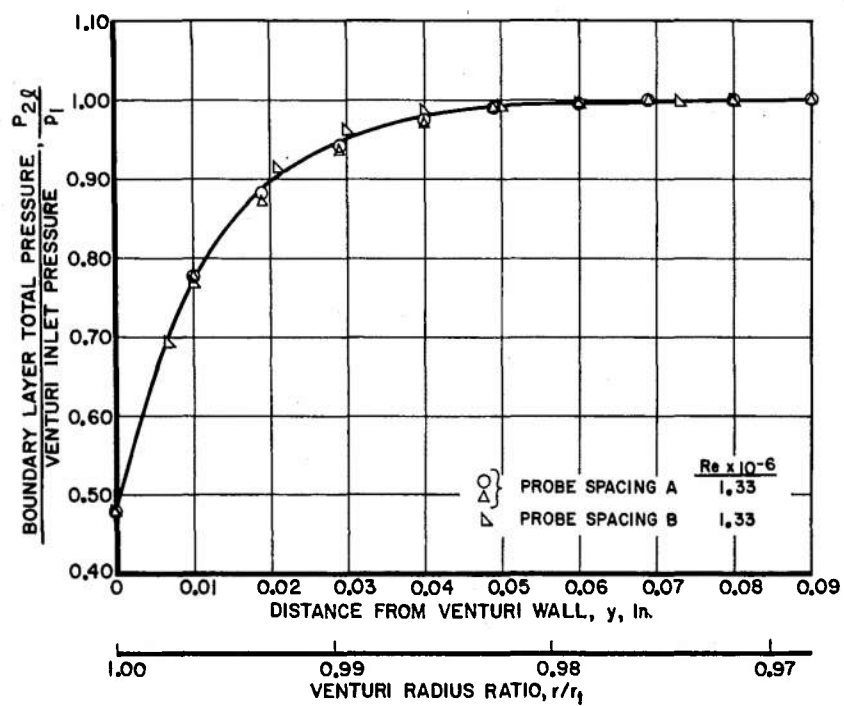


Fig. 18 Total Pressure Profiles at Venturi Inlet

a. Boundary Layer Total Pressure at $\gamma = 0.010$ in.

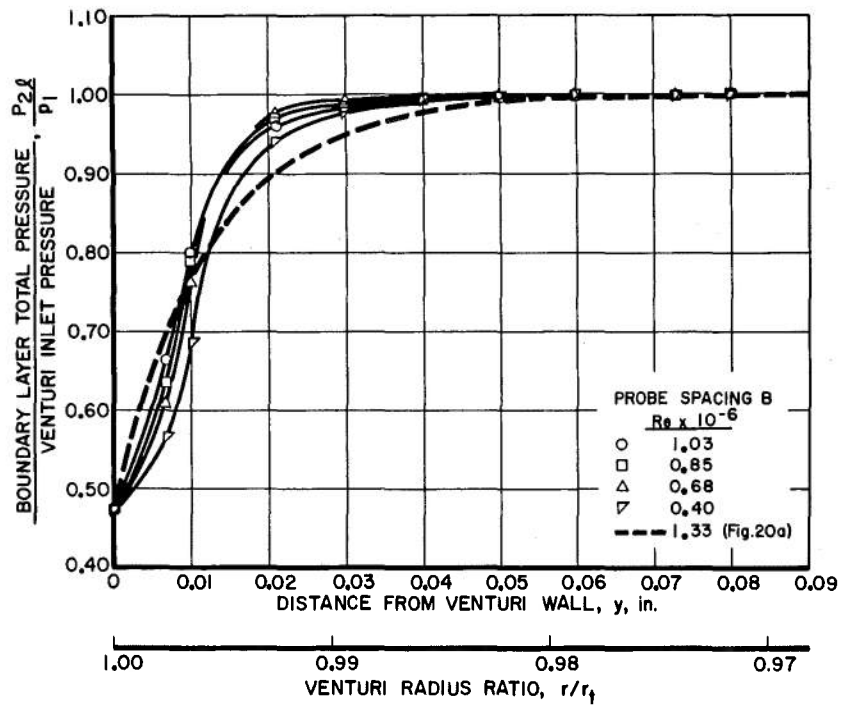
b. Venturi Throat Wall Static Pressure

Fig. 19 Variation of Venturi Throat Conditions as a Function of Overall Venturi Pressure Ratio

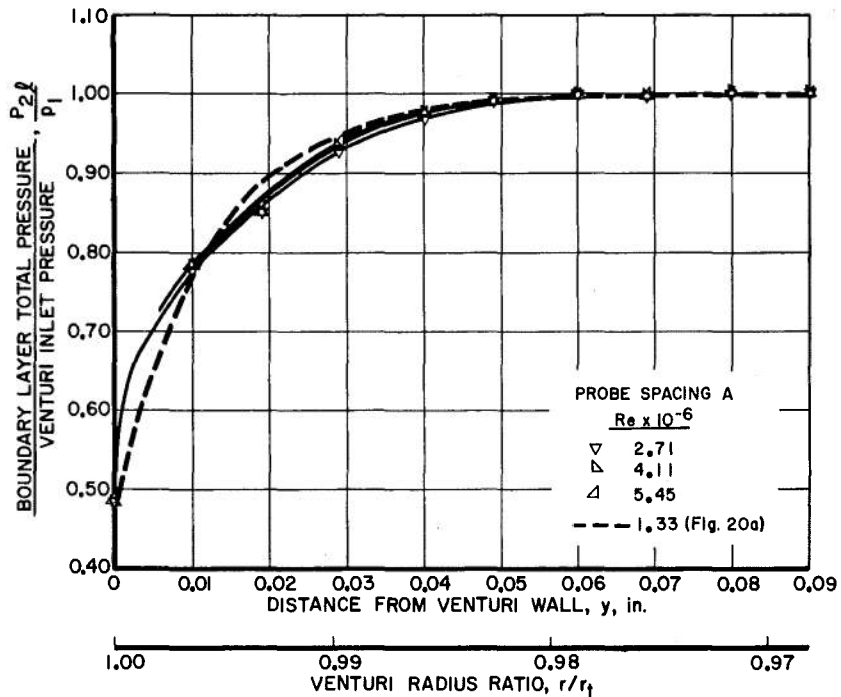


a. Different Probe Spacings

Fig. 20 Venturi Throat Boundary Layer Total Pressure Profiles

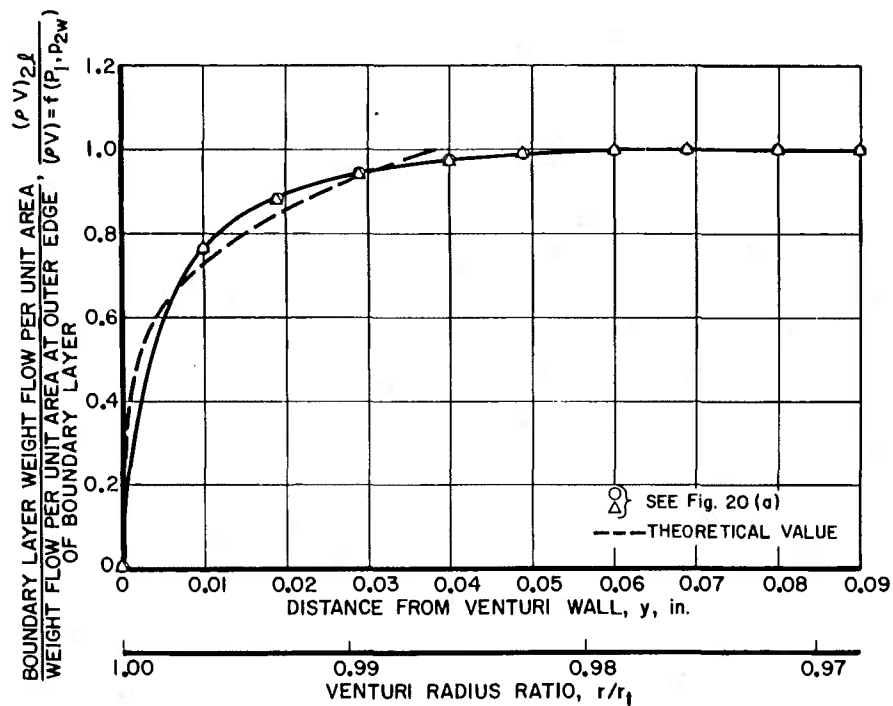


b. Reynolds Number Range: 0.40×10^6 to 1.03×10^6

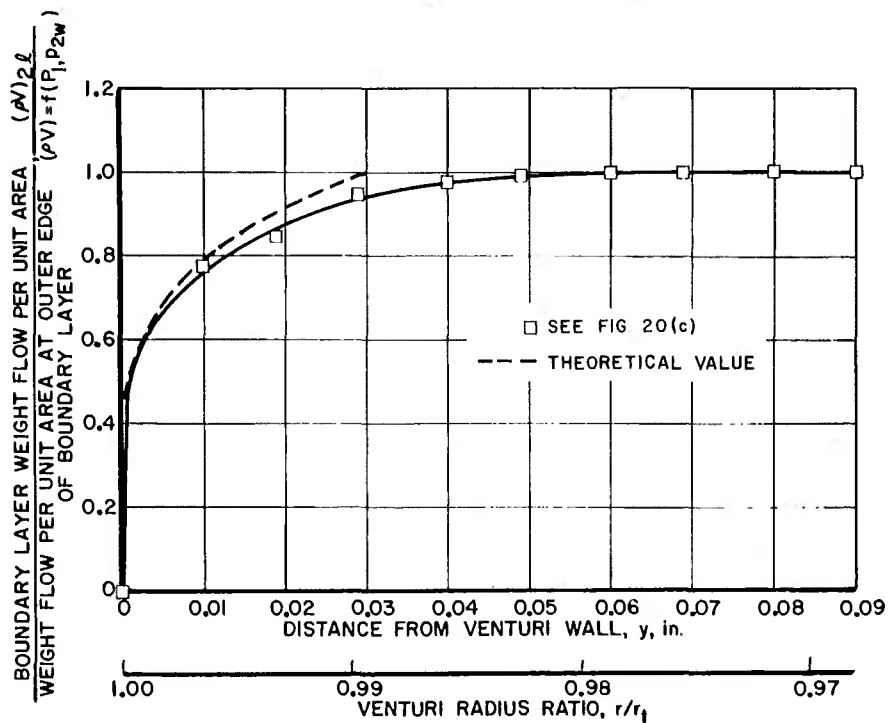


c. Reynolds Number Range: 2.71×10^6 to 5.45×10^6

Fig. 20 Concluded



a. $Re = 1.33 \times 10^6$



b. $Re = 5.45 \times 10^6$

Fig. 21 Comparison of Theoretical and Experimental Boundary Layer Weight-Velocity Profiles

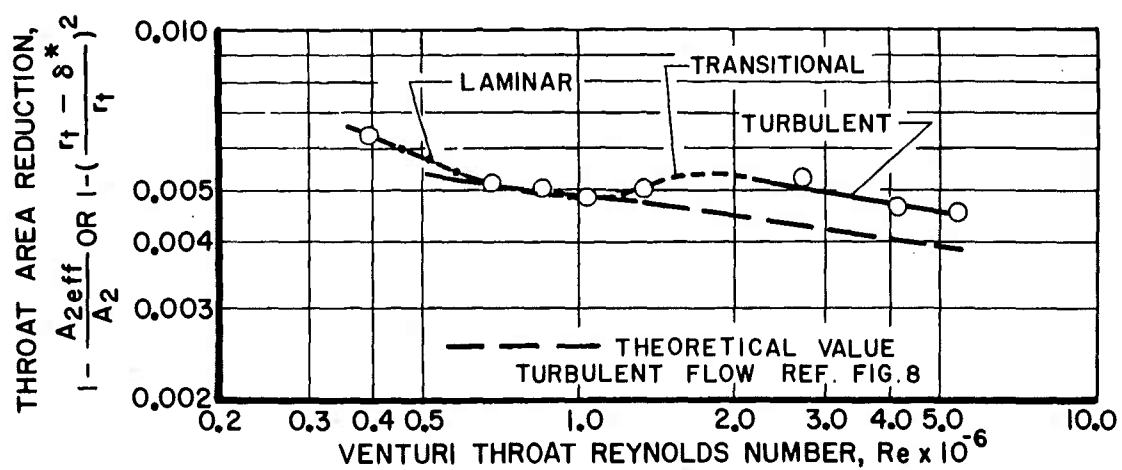
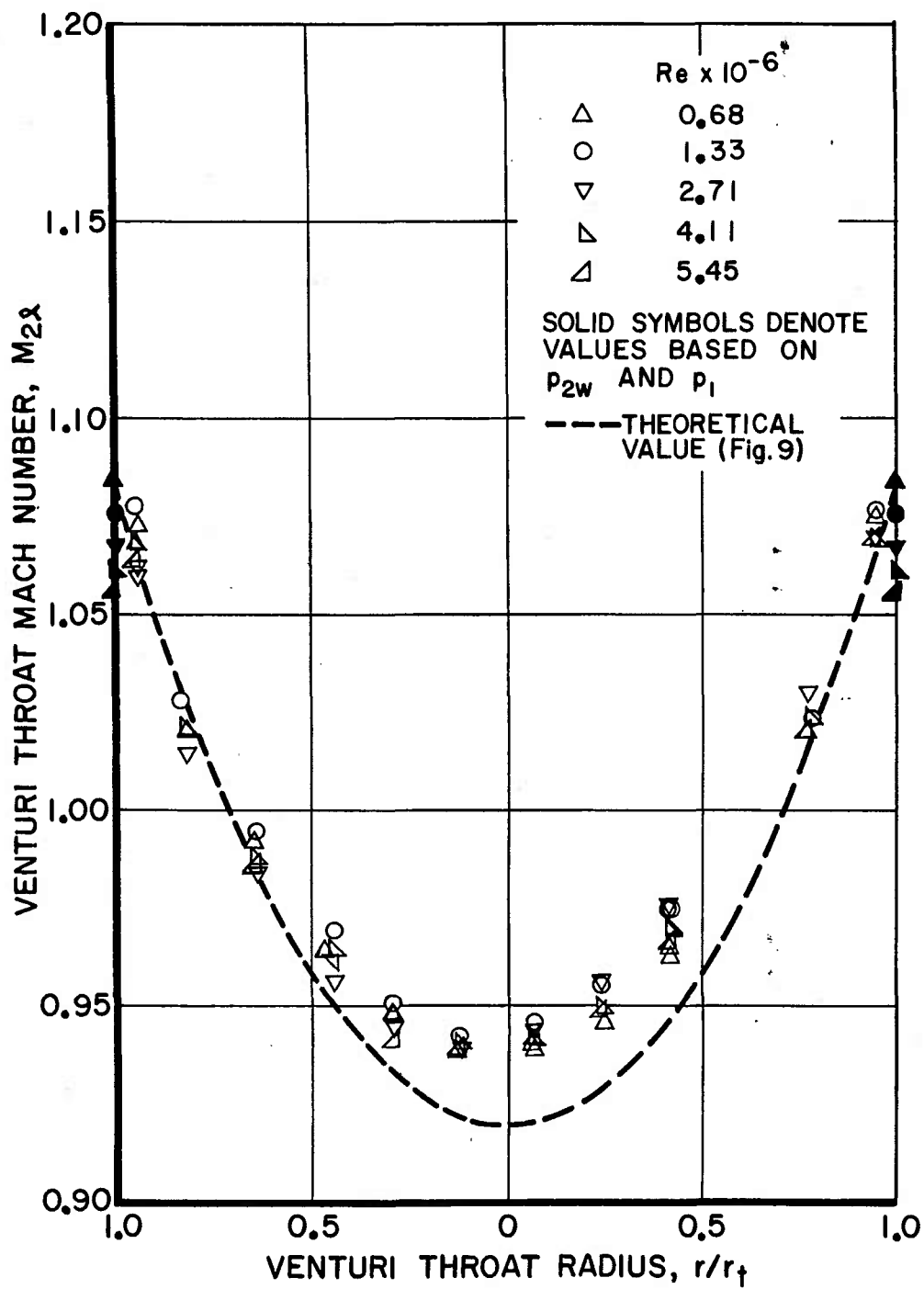
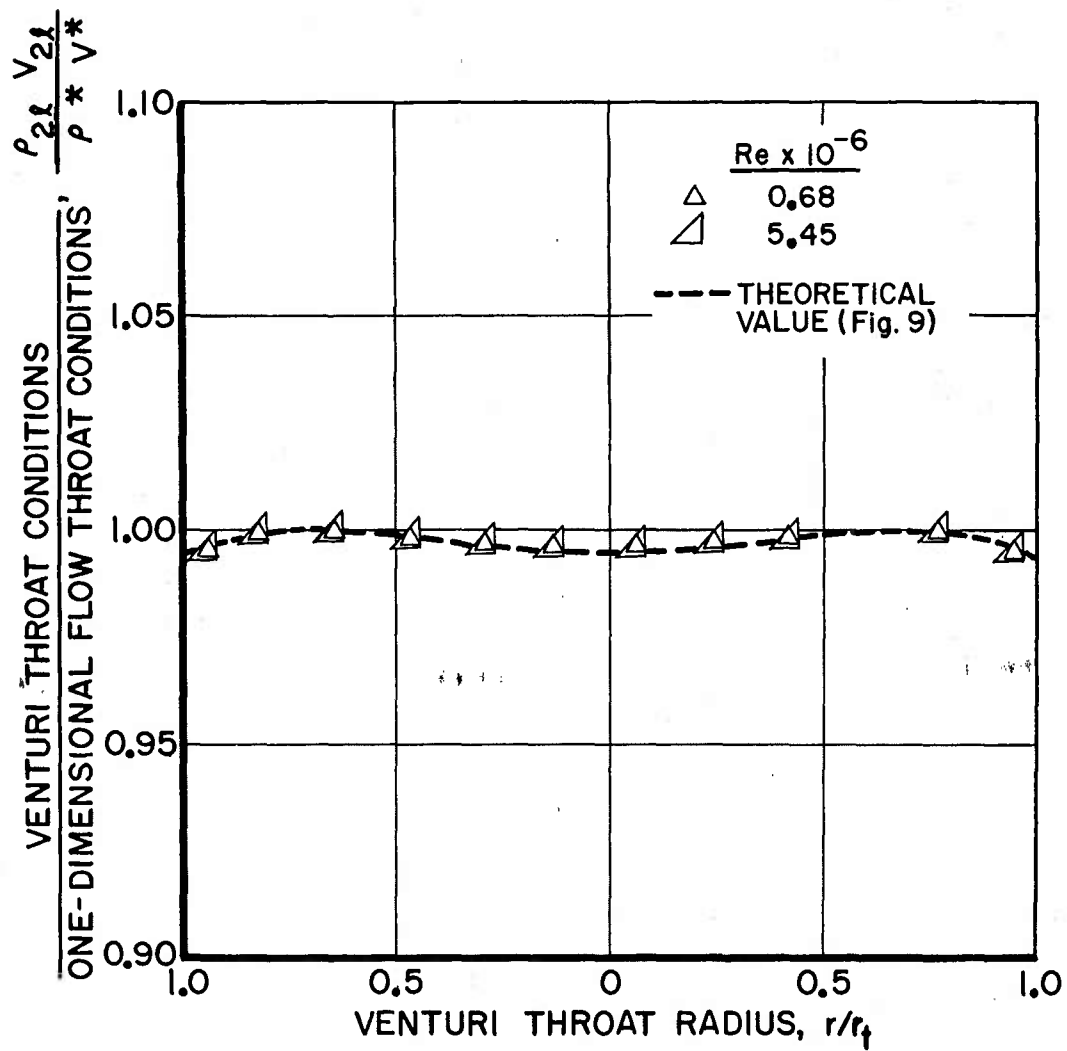


Fig. 22 Comparison of Theoretical and Experimental Venturi Effective Throat Area Reduction Resulting from Boundary Layer Effects



a. Mach Number

Fig. 23 Comparison of Theoretical and Experimental Mach Number and Weight-Velocity Profiles across Venturi Throat



b. Weight-Velocity

Fig. 23 Concluded

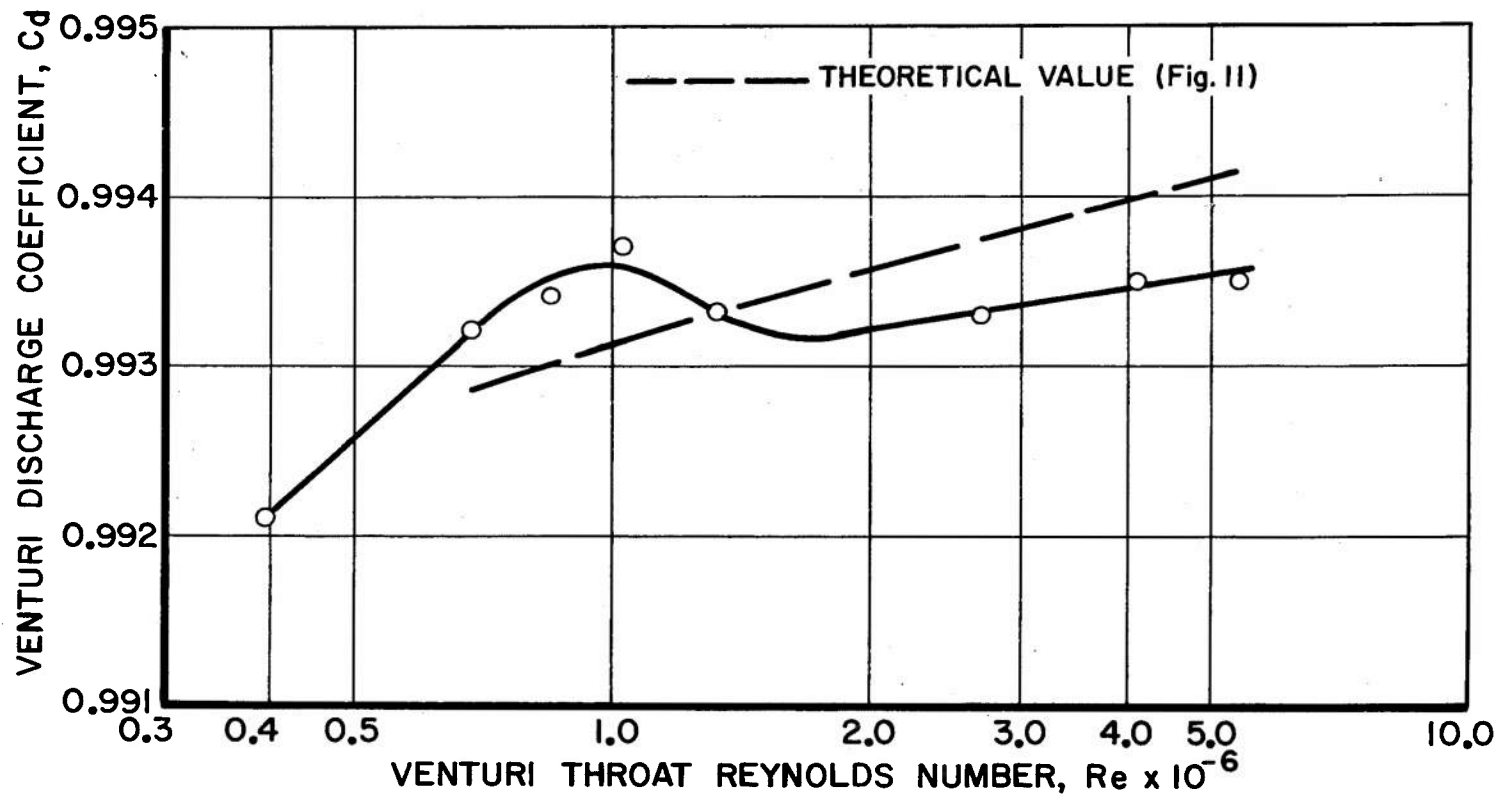


Fig. 24 Comparison of Theoretical and Experimental Venturi Discharge Coefficients